Accepted Manuscript

Heterotrimeric G Stimulatory Protein alpha subunit is Required for Intestinal Smooth Muscle Contraction in Mice

Xiaoteng Qin, Shangming Liu, Qiulun Lu, Meng Zhang, Xiuxin Jiang, Sanyuan Hu, Jingxin Li, Cheng Zhang, Jiangang Gao, Min-Sheng Zhu, Yun Zhang, Wencheng Zhang

PII: S0016-5085(16)35531-7
DOI: 10.1053/j.gastro.2016.12.017
Reference: YGAST 60878

To appear in: *Gastroenterology*
Accepted Date: 21 December 2016

Please cite this article as: Qin X, Liu S, Lu Q, Zhang M, Jiang X, Hu S, Li J, Zhang C, Gao J, Zhu M-S, Zhang Y, Zhang W, Heterotrimeric G Stimulatory Protein alpha subunit is Required for Intestinal Smooth Muscle Contraction in Mice, *Gastroenterology* (2017), doi: 10.1053/j.gastro.2016.12.017.

Heterotrimeric G Stimulatory Protein alpha subunit is Required for Intestinal Smooth Muscle Contraction in Mice

Xiaoteng Qin[1], Shangming Liu[1,2], Qiulun Lu[3], Meng Zhang[1], Xiuxin Jiang[4], Sanyuan Hu[4], Jingxin Li[5], Cheng Zhang[1], Jiangang Gao[6], Min-Sheng Zhu[7], Yun Zhang[1*] and Wencheng Zhang[1*]

[1] The Key Laboratory of Cardiovascular Remodeling and Function Research, Chinese Ministry of Education and Chinese Ministry of Health; The State and Shandong Province Joint Key Laboratory of Translational Cardiovascular Medicine, Qilu Hospital of Shandong University, Jinan, China; [2]Key Laboratory of the Ministry of Education for Experimental Teratology, Department of Histology and Embryology, Shandong University School of Medicine, Jinan, China; [3]Key Laboratory of Molecular Biophysics of the Ministry of Education, College of Life Science and Technology and Center for Human Genome Research，Huazhong University of Science and Technology, Wuhan, China; [4]Department of General Surgery, Qilu Hospital of Shandong University, Jinan, China; [5]Department of Physiology, School of Medicine, Shandong University, Jinan, China; [6]School of Life Science and Key Laboratory of the Ministry of Education for Experimental Teratology, Shandong University, Jinan, China; [7]State Key Laboratory of Pharmaceutical Biotechnology and Model Animal Research Center and MOE Key Laboratory of Model Animal for Disease Study, Nanjing University, Nanjing, China.

Short title: Heterotrimeric G Stimulatory Protein alpha subunit regulates Contractility

Grant Support: This work was supported by grants from the Taishan Scholar Project of Shandong Province of China (tsqn20161066 to W. Z.), the National Natural Science Foundation of China (81570393 to W. Z., 81425004, 91339109 and 81270350 to C. Z., 31400771 to M. Z.), the Natural Science Foundation of Shandong Province (ZR2015HM002 to W. Z.), the Program of Introducing Talents of Discipline to Universities (B07035 to Y. Z.), the State Program of National Natural Science Foundation of China for Innovative Research Group (81321061 to Y. Z.), the State Key Program of National Natural Science of China (61331001 and 81530014 to Y. Z.) and the International Collaboration and Exchange Program of China (81320108004 to Y. Z.).

Conflicts of interest: There are no conflicts of interest to disclose.

Author Contributions: X. Q., S. L. and M. Z. designed and performed the experiments, analyzed data, and prepared the manuscript; Q. L. and X. J. performed statistical analysis; S. H. and J. L. performed data analysis and interpretation; J. G. and M.-S. Z. provided mice; C. Z., Y. Z. and W. Z. obtained funding; W. Z. conceived the projects, designed the experiments, reviewed the data, and wrote the manuscript.

*To Whom Correspondence Should be addressed:

Wencheng Zhang, Ph.D or Yun Zhang, MD, Ph.D

Qilu Hospital of Shandong University

No. 107, Wen Hua Xi Rd, Jinan, Shandong, China. 250012

E-mail: zhangwencheng@sdu.edu.cn or zhangyun@sdu.edu.cn

Phone: 86-531-82169258

Abbreviations used in this paper:

AC, adenylyl cyclase

ACh, acetylcholine

ACTA2, actin, alpha 2, smooth muscle, aorta

cAMP, cyclic adenosine monophosphate

ChIP, Chromatin immunoprecipitation

CIP, chronic intestinal pseudo-obstruction

CRE, cAMP response element

CREB1, cAMP response element binding protein 1

EFS, electrical field stimulation

Fox, Foxo family of forkhead

GNAS, guanine nucleotide binding protein, alpha stimulating

Gsa, heterotrimeric G stimulatory protein alpha subunit

KO, knockout

ISO, isoproterenol

MLCK, myosin light chain kinase

MYH11, myosin heavy chain 11

PKA, protein kinase A

SMC, smooth muscle cell

SRF, serum response factor

Abstract:

Background & Aims: The alpha subunit of the heterotrimeric G stimulatory protein (Gsa), encoded by the guanine nucleotide binding protein, alpha stimulating gene (*Gnas*, in mice), is expressed ubiquitously and mediates receptor-stimulated production of cyclic adenosine monophosphate (cAMP) and activation of the protein kinase A signaling pathway. We investigated the roles of Gsa *in vivo* in smooth muscle cells of mice. **Methods**: We performed studies of mice with Cre recombinase-mediated disruption of *Gnas* in smooth muscle cells (Gsa^{SMKO} and SM22-$CreER^{T2}$, induced in adult mice by tamoxifen). Intestinal tissues were collected for histologic, biochemical, molecular, cell biology, and physiology analyses. Intestinal function was assessed in mice using the whole-gut transit time test. We compared gene expression patterns of intestinal smooth muscle from mice with *vs* without disruption of *Gnas*. Biopsy specimens from ileum of patients with chronic intestinal pseudo-obstruction and age-matched control biopsies were analyzed by immunohistochemistry. **Results**: Disruption of *Gnas* in smooth muscle of mice reduced intestinal motility and led to death within 4 weeks. Tamoxifen-induced disruption of *Gnas* in adult mice impaired contraction of intestinal smooth muscle and peristalsis. More than 80% of these died within 3 months of tamoxifen exposure, with features of intestinal pseudo-obstruction characterized by chronic intestinal dilation and dysmotility. Gsa deficiency reduced intestinal levels of cAMP and transcriptional activity of the cAMP response element binding protein 1 (CREB1); this resulted in decreased expression of the forkhead box F1 gene (*Foxf1*) and protein, and contractile

proteins such as myosin heavy chain 11 (MYH11); actin, alpha 2, smooth muscle, aorta (ACTA2); calponin 1 (CNN1); and myosin light chain kinase (MLCK). We found decreased levels of Gsa, FOXF1, CREB1, and phosphorylated CREB1 proteins in intestinal muscle layers of patients with chronic intestinal pseudo-obstruction, compared with tissues from controls. **Conclusions**: Gsa is required for intestinal smooth muscle contraction in mice, and its levels are reduced in ileum biopsies of patients with chronic intestinal pseudo-obstruction. Mice with disruption of *Gnas* might be used to study human chronic intestinal pseudo-obstruction.

KEY WORDS: mouse model, CIP, intestine, digestion

Introduction

Smooth muscle cells (SMCs) are the primary contractile components of digestive, cardiovascular, respiratory and genitourinary systems. Contractile dysfunction of SMCs is associated with various diseases including chronic intestinal pseudo-obstruction (CIP), atherosclerosis, hypertension and asthma. The main feature of these diseases is decreased expression of proteins required for normal SMC contractile function [1]. Therefore, we need to understand the mechanisms that control the expression of contractile and regulatory proteins in SMCs, to determine how these processes are altered in pathological conditions.

Many studies have identified that transcription factors such as serum response factor (SRF) and the Foxo family of forkhead (Fox) proteins control the expression of contractile proteins in SMCs [2]. Knockout of SRF in intestinal SMCs of adult mice attenuated the expression of smooth muscle-specific genes and resulted in a phenotype of CIP [3-4]. Foxf1 binds to SRF and Myocd to regulate the expression of contractile proteins, and Foxf1 deletion in SMCs results in reduced contractile protein expression and impaired colonic contractility [5].

The heterotrimeric G-protein alpha subunit (Gsa) is encoded by guanine nucleotide binding protein, alpha stimulating (GNAS) (Gnas in mice), which is ubiquitously expressed in many cell types and responsible for receptor-stimulated cyclic adenosine monophosphate (cAMP) generation and activation of the protein kinase A (PKA) pathway [6]. PKA can phosphorylate various downstream targets that are involved in a number of pathways. For example, PKA phosphorylates cAMP

response element binding protein 1 (CREB1) at Ser 133, to induce the expression of CREB1 target genes [7]. Accumulating evidence has demonstrated that aberrant expression of Gsa leads to various dysfunctions in cell growth, proliferation, apoptosis, differentiation, and metabolism [8]. Adipose tissue-specific disruption of Gsa results in a severely lean phenotype and early mortality [9]. Chondrocyte-specific ablation of Gsa leads to growth-plate defects and hypertrophic differentiation of growth-plate cartilage [10]. Recent studies have shown mutations in GNAS related to many human diseases: heterozygous mutation for loss of function in GNAS leads to Albright hereditary osteodystrophy [11], whereas mutation activating GNAS results in McCune–Albright syndrome [12]. However, the roles of Gsa in SMCs have not been investigated.

In the present study, we examined the potential function of Gsa in SMCs by using mice with Acta2-Cre– or SM22-CreER^{T2}–mediated Gsa knockout (KO). Acta2-Cre–mediated Gsa KO (Gsa^{SMKO}) in smooth muscle reduced intestinal motility and led to early death, before 4 weeks. SM22-CreER^{T2}–mediated Gsa KO induced by tamoxifen in adult mice (adult Gsa^{SMKO}) impaired the contraction of intestinal smooth muscle and resulted in a phenotype similar to CIP. CIP is characterized by chronic intestinal dilation and dysmotility in the absence of mechanical obstruction [13]. These results demonstrate that Gsa plays a critical function in intestinal motility in mice.

Materials and Methods

Generation of Smooth Muscle-specific Gsa KO Mice

To ablate Gsa specifically in smooth muscle (Gsa^{SMKO}), $Gsa^{fl/fl}$ mice [14] were crossed with Acta2-Cre mice that express Cre recombinase under the control of the Acta2 promoter [15]. To generate adult smooth muscle-specific Gsa KO mice (adult Gsa^{SMKO}), $Gsa^{fl/fl}$ mice were crossed with SM22-$CreER^{T2}$ mice expressing a tamoxifen-inducible Cre recombinase under control of the SM22 promoter [16]. Tamoxifen (1 mg/day) was injected intraperitoneally for five consecutive days. All experiments were conducted in accordance with the guidelines of the Animal Care and Use Committee of Shandong University.

Analysis of Smooth Muscle Contractility

Force measurements were performed as described [17]. The mice were killed by cervical dislocation. Segments (6 mm long) of the jejunum and ileum were mounted in a 37°C organ bath and tied with surgical silk to the hooks of a force transducer (MLT0202; AD Instruments) and length-adjusting micrometer. After equilibrating in H-T buffer (137.0 mmol/L NaCl, 2.7 mmol/L KCl, 1.0 mmol/L $MgCl_2$, 1.8 mmol/L $CaCl_2$, 10 mmol/L HEPES, and 5.6 mmol/L glucose, pH 7.4) for 15 min, the contractile effect of KCl (87 mM), ACh (1 mM) and electrical field stimulation (EFS) (20 Hz, 30 V, pulse train, 20 s) was investigated.

Whole-gut Transit Time Test

To determine intestinal function, a whole-gut transit time test was performed with minor modification [18]. We injected 100 μl of charcoal test meal (5% [w/v] charcoal in 0.9% NaCl) by orogastric gavage and monitored feces for the first appearance of black dye.

Human Cases

Full-thickness biopsy specimens were obtained from five female patients with a mean age of 51.2 ± 8.3 years who met the criteria for CIP. Age matched female control specimens were obtained from patients (mean age: 50.3 ± 9.2 years) with diseases unrelated to gastrointestinal motility disorders. The use of human tissues was approved by the Medical Institutional Ethics Committee of Qilu Hospital, Shandong University, China.

Statistical analysis

Data are expressed as mean ± SEM and were analyzed by using GraphPad Prism 3 (GraphPad Software Inc., San Diego, CA). Statistical comparisons between 2 groups involved Student's *t* test and otherwise by two-way ANOVA and Bonferroni post-tests. $P < 0.05$ was considered statistically significant.

Results

Gsa deficiency in smooth muscle results in postnatal lethality

To elucidate the biological significance of Gsa expression in smooth muscle *in vivo*, $Gsa^{flox/flox}$ mice were crossbred with Acta2-Cre mice to generate $Gsa^{flox/+}$*/Acta2-Cre* mice, which were further intercrossed to obtain $Gsa^{flox/flox}$*/Acta2-Cre* mice (Gsa^{SMKO} mice) (Figure 1A). The littermate $Gsa^{flox/flox}/Cre^{-}$ mice were used as controls. Immunohistochemistry showed nuclear localization of Cre in the smooth muscle layer of jejunum and ileum from Acta2-Cre mice (Figure 1B), suggesting Acta2-Cre-mediated recombination happening in the smooth muscle

of jejunum and ileum. Western blots confirmed significantly reduced Gsa expression in the muscle of the jejunum, ileum and aorta of Gsa^{SMKO} mice (Figure 1C). Immunohistochemistry further demonstrated Gsa deletion in the smooth muscle cells of aorta, jejunum and ileum from the Gsa^{SMKO} mice (Supplementary Figure 1A to 1C). However, Gsa levels were not changed in the non-smooth muscle tissues such as brain, skeletal muscle and skin from control and Gsa^{SMKO} mice (Figure 1D).

Gsa^{SMKO} pups were born at the expected Mendelian ratio. At birth, the size and weight of Gsa^{SMKO} mice was comparable to that of their control littermates, but postnatal growth was retarded. From day 10 after birth, all Gsa^{SMKO} mice showed significantly reduced body weight relative to their controls (Figure 1E). At day 21, male Gsa^{SMKO} mice weighed 34.1% less than their controls (7.16 ± 1.04 g vs. 10.86 ± 0.92 g, $n = 6$; $P < 0.01$). Importantly, Gsa^{SMKO} mice began to die at day 14 after birth. None of the Gsa^{SMKO} mice survived beyond postnatal day 28, whereas all control pups survived (Figure 1F). These data suggest that smooth muscle Gsa is essential for growth, and deficiency of Gsa can lead to serious growth retardation and early mortality. However, the detailed reason for the death of Gsa^{SMKO} mice is not clear.

Contraction was impaired in Gsa^{SMKO} smooth muscles

To evaluate the effects of Gsa deletion on intestinal motility, we measured rhythmic contractions of the jejunum and ileum from control and Gsa^{SMKO} mice at 3 weeks of age. Peristaltic contractile tension of jejunum and ileum from Gsa^{SMKO} mice was significantly decreased as compared with controls (Figure 2A). At necropsy, the whole digestive tract from 3-week-old Gsa^{SMKO} mice appeared normal, including the

small intestine. Histologic examination showed comparable thickness of the Gsa-deficient and control ileal or jejunal muscle layers (Figure 2B).

To determine the contractile properties of Gsa-deficient smooth muscle, we measured the tension in isolated strips in response to KCl or the muscarinic agonist, ACh. Jejunal strips from Gsa^{SMKO} mice at 3 weeks of age showed only 38.2% of the tension of control tissue in response to KCl (Figure 2C). Similar results were obtained with ileal tissues (Figure 2D). As well, intestinal smooth muscles for both jejunum and ileum from Gsa^{SMKO} mice showed only 35.7% to 43.0% of the tension of control tissue in response to ACh (Figure 2C and 2D). We also investigated the responses to EFS used to release ACh from parasympathetic nerves intrinsic in isolated tissues. The contraction forces obtained with EFS in jejunal or ileal smooth muscle were significant reduced after Gsa knockout (Figure 2E). More importantly, intestinal contraction was impaired even in both jejunum and ileum from Gsa^{SMKO} mice at 13 days of age (Supplementary Figure 2A and 2B). Therefore, Gsa plays a important role in normal intestinal smooth muscle contractions.

Smooth muscle-specific Gsa deletion in adult mice confers severe intestinal obstruction

To explore the roles of smooth muscle Gsa in adult mice *in vivo*, $Gsa^{lox/flox}$ mice were cross-bred with SM22-$CreER^{T2}$ mice expressing a tamoxifen-activated Cre recombinase to ablate Gsa expression in adult smooth muscle (adult Gsa^{SMKO}; Figure 3A). We used $Gsa^{flox/flox}/Cre^{-}$ mice with tamoxifen injection as controls. Immunohistochemistry demonstrated Gsa deletion in the smooth muscle cells of

jejunum and ileum from the adult Gsa^{SMKO} mice (Supplementary Figure 1D and 1E).

Control and adult Gsa^{SMKO} mice were monitored at various times after tamoxifen injection to determine the pathologic phenotype. From 28 days after the first tamoxifen injection, the body weight was lower for adult Gsa^{SMKO} than control mice (Figure 3B). From 3 weeks after tamoxifen injection, adult Gsa^{SMKO} mice showed reduced physical body motility (data not shown). The lower abdomen started to bloat and increase in volume, and adult Gsa^{SMKO} mice began to die (Figure 3C). During this period, intake of food and excretion of feces were markedly reduced (Figure 3D). We found more than 80% lethality within 3 months after the first application of tamoxifen (Figure 3C). In contrast, tamoxifen-treated *Gsa*$^{flox/flox}$/*Cre*$^{-}$ control mice appeared normal, with no deaths. In all adult Gsa^{SMKO} mice, gross necropsy showed severe intestinal situs with extremely dilated and food-filled ileum (Figure 3E). Motility of the intestine was determined by functional assays. Charcoal, a black dye, was injected into the stomach and stool was monitored. Despite a comparable length of the intestinal tract, adult Gsa^{SMKO} mice showed about three-fold longer whole-gut transit time than control mice (Figure 3F). Adult Gsa^{SMKO} mice may develop a severe motility disorder similar to some symptoms of human patients with CIP, leading to cachexia and death.

Gsa deficiency in adult SM impairs contractile activity

Histologic analyses showed marked changes in the intestinal tract of adult Gsa^{SMKO} mice (Figure 4A and B). At three weeks after tamoxifen injection, the small intestine was dilated, with the mean diameter significantly increased (1.6±0.3-fold)

for the ileum as compared with controls (3566±1011 μm vs 2254±562 μm; $p<0.05$). The mean diameter of the jejunum did not change significantly (1.1±0.2-fold; 2890±539 μm vs 2540±149 μm; p=0.156). However, the cross-sectional thickness of the ileal muscle layer was increased (2.4±0.5-fold for the longitudinal muscle layer and 2.1±0.4-fold for the circular muscle layer; $p<0.05$), whereas the thickness of jejunal muscle was not altered (1.2±0.2-fold for longitudinal muscle and 1.3±0.3-fold for circular muscle; $p>0.05$). Inspection of intestinal cross sections showed noticeably enlarged muscle cells. The number of nuclei in an arc of the ileal wall equal to one-tenth the circumference did not differ between adult Gsa^{SMKO} and control mice (longitudinal muscle: 120±20 vs 116±15, p=0.69; circular muscle: 114±9 vs 109±8, p=0.77). Thus, the thicker muscle layers were due largely to SMC hypertrophy.

Gsa knockout in intestinal smooth muscle did not affect the levels of β-adrenergic receptors (ADRB1 and ADRB2) (Supplementary Figure 3A and 3B). Contractile functions of the intestinal tunica muscularis were tested by tension recordings of smooth muscle tissues (jejunum and ileum). The tension responses to KCl in adult Gsa^{SMKO} muscle was only about 25% of that observed in control muscle (jejunum, 34.3% and ileum, 15.4%). Similar results were obtained with ACh (Figure 4C and 4D) and EFS (Figure 4E). These data clearly indicate that Gsa regulates depolarization- and agonist-mediated intestinal smooth muscle contractions.

Gsa deletion reduced the expression of contractile proteins and cAMP/CREB1 signaling

We performed a genome-wide microarray assay of control and Gsa-deficient

intestinal smooth muscle to profile differentially expressed genes that might be involved in Gsa regulation. As shown in Figure 5A and Supplementary Table 1, we found 1165 genes with >2.0-fold upregulation and 904 genes with > 2-fold downregulation in 3 independent experiments. To understand some important biological processes affected by Gsa in smooth muscle cells, a Gene ontology analysis was performed and revealed Gsa roles in the regulation of transcription, phoshorylation, cell proliferation, cell cycle, cell differentiation, cell adhesion, cell migration and immune response (Figure 5B). Pathway analysis with the KEGG database further classified the functional annotations of genes and revealed upregulated and downregulated genes significantly enriched in top 10 pathways (Figure 5C). To verify the microarray analysis data, we examined differentially expressed genes that are involved in smooth muscle contraction from control and adult Gsa^{SMKO} mice at three weeks after tamoxifen injection. The mRNA levels of contractile proteins including myosin heavy chain 11 (MYH11), actin, alpha 2, smooth muscle, aorta (ACTA2), calponin 1 (CNN1) and myosin light chain kinase (MLCK) were significantly reduced in the Gsa-deficient jejunum (Figure 5D), which were further confirmed by western blot analysis (Supplementary Figure 3A and 3B). In analyzing transcription factors that control the expression of contractile proteins in SMCs, serum response factor (SRF) mRNA levels were not changed in the Gsa-deficient jejunum. However, Myocd mRNA levels were slightly decreased and Foxf1 mRNA levels were significantly reduced with Gsa deletion (Figure 5D), which was further confirmed by western blot analysis (Figure 5F).

Because Gsa is responsible for receptor-stimulated cAMP generation and subsequent CREB1 activation, we measured cAMP levels and CREB1 activity with Gsa KO. As expected, Gsa KO reduced cAMP levels in basal or response to isoproterenol (ISO) (Figure 5E). Both phospho-CREB1 at Ser 133 and total CREB1 levels were significantly reduced with Gsa KO (Figure 5F), ISO-induced CREB1 phosphorylation was also decreased in Gsa-deficient smooth muscle (Figure 5E). Our data suggest that Gsa KO results in reduced cAMP/CREB1 signaling and expression of contractile proteins, thereby impairing smooth muscle contraction.

CREB1 binds with Foxf1 promoter and regulates its expression

We next dissected how Gsa/CREB1 regulates Foxf1 expression. We analyzed the promoter of Foxf1 by using the Transcription Factor Database (http://jaspar.genereg.net), an Internet-based transcription-factor binding-site program. One CRE site was found in the Foxf1 promoter (Figure 6A), so CREB1 may bind to the Foxf1 promoter and regulate its expression. The cAMP activator forskolin, used to induce CREB1 activity, could increase Foxf1 expression in intestinal SMCs (Figure 6B).

To confirm that CREB1 can bind to the Foxf1 promoter, we used ChIP assay. Forskolin induced the binding of CREB1 to the CRE site in the Foxf1 promoter (Figure 6C). To further analyze the role of the CREB1 binding site on Foxf1 promoter activity, we mutated the core CREB1 binding site in CRE and then inserted it into a luciferase plasmid. Forskolin significantly increased luciferase activity from the WT but not CRE-mutant Foxf1 promoter (Figure 6D). Therefore, CREB1 binds with the

Foxf1 promoter and regulates its expression.

Levels of Gsa, Foxf1 and p-CREB1/CREB1 were reduced in the intestinal muscle layer of patients with CIP

A genome-wide microarray assay of intestinal smooth muscle from patients with CIP and age-matched control was conducted to profile differentially expressed genes. As shown in Supplementary Figure 4A and Supplementary Table 2, we found 125 genes with >2.0-fold upregulation and 111 genes with > 2-fold downregulation in CIP group compared with control group. Pathway analysis with the KEGG database classified the functional annotations of genes and revealed upregulated and downregulated genes significantly enriched in top 9 pathways (Supplementary Figure 4B). There are 2069 differentially expressed genes from Gsa knockout group. The human CIP group and Gsa knockout group shared 48 common differentially expressed genes (Supplementary Figure 4C), of which 21 genes were upregulated and 27 genes including Gsa, CREB1, Foxf1 and contractile proteins were downregulated (Supplementary Figure 4D and 4E). Thus, the phenotype of the adult Gsa^{SMKO} mice shares some aspects of CIP pathology in humans.

To further confirm the expression of Gsa/CREB1/Foxf1 signaling in intestines of patients with CIP, immuno-histological staining was performed. Compared with control intestinal muscle layers, layers of patients with CIP showed significantly reduced levels of Gsa, Foxf1 and p-CREB1/CREB1 (Figure 7A and 7B), which indicates the important role of Gsa/CREB1/Foxf1 signaling in the development of human chronic intestinal pseudo-obstruction.

Discussion

To determine the role of Gsa in SMCs *in vivo*, we generated two kinds of smooth muscle-specific Gsa-KO mice in different Cre recombinase mice. Acta2-Cre-mediated Gsa KO resulted in reduced intestinal contraction and early death before 4 weeks for unknown reasons. Adult Gsa-KO mice were induced with time-controlled recombination by tamoxifen. Gsa KO in adult SMCs led to dilation and impaired contraction of the intestine, which resulted in defective peristalsis *in vivo* and most death within 3 months; both toxicity and malnutrition were assumed to be the probable cause of death. In the molecular mechanism, Gsa regulates the expression of contractile proteins through cAMP/CREB1-mediated Foxf1 and thus plays an important role in normal intestinal smooth muscle contraction (Figure 7C). Our study revealed the roles of smooth muscle Gsa at the animal level, which will increase our understanding of Gsa multi-functions.

The phenotype of Gsa-KO mice is caused by decreased Foxf1 expression. Foxf1 has been identified as an important transcription factor for the SMC genes encoding the main effectors of contraction [5]. Foxf1 binds to SRF and Myocd to regulate the expression of smooth-muscle contractile proteins. Smooth muscle-specific Foxf1 deletion results in neonatal lethality and impaired contractility [5]. Other transcription factors such as SRF, GATA6 and MEF2 also play a role in regulating SMC gene expression [19]. Smooth muscle-specific SRF mice showed a similar phenotype as our adult Gsa^{SMKO} mice [3-4]. Recent studies also showed downregulated SMC-specific markers in various motility disorders in humans. For

example, the jejunal circular smooth muscle layer showed no ACTA2 expression in idiopathic forms of CIP [20]. MYH11 was downregulated in colon biopsy specimens of patients with idiopathic megacolon and slow-transit constipation [21]. Similarly, Gsa^{SMKO} mice showed intestinal motility dysfunction accompanied by downregulation of SMC-specific markers such as ACTA2 and MYH11.

Gsa deletion in intestinal smooth muscle resulted in decreased contractile responses. Gsa-deficient muscle strips displayed much lower contractile force than control strips, independent of the agonist applied. The main cause is presumably changes in the contractile machinery of intestinal smooth muscle because key downstream regulators such as MLCK and effectors of contraction such as ACTA2 and MYH11 are downregulated in Gsa-deficient SMCs. However, Gsa-dependent cAMP signaling contributes to smooth muscle relaxation [22]. The different conclusions are explained by different research methods. The previous study used chemical regents to elevate cAMP levels to explore its function, which were transient and sometimes not specific. In our mouse KO model, long-term deletion of Gsa caused changes in downstream regulators including phospho-CREB1 (Ser 133) and total CREB1, which downregulated smooth-muscle contractile proteins and reduced contractility.

Reduced contractility with Gsa deficiency has significant consequences for the intestinal performance. The retarded passage of charcoal showed that whole-gut transit time was approximately three-fold increased as compared with controls. Furthermore, the dilated intestine in adult Gsa^{SMKO} mice may result from chronic

pseudo-obstruction associated with hypertrophy of the smooth muscle in the intestinal wall, which is likely an adaptive response to increased workload of smooth muscle with the diminished contractility.

CIP may be congenital or acquired secondary to other disorders, such as postoperative ileus and autoimmune or infectious diseases [4]. A proper diagnosis and treatment of this rare and disabling disorder is difficult because the underlying pathology is poorly understood. CIP can be classified as neuropathic or myopathic forms based on histopathology data and patterns of motility disorder [23]. Smooth muscle myopathies may be responsible for the disease in approximately one third of cases of congenital CIP [24]. In this study, we describe a mouse model of adult smooth muscle-specific Gsa KO that displays clinical manifestations similar to CIP. Moreover, we report on the reduced levels of Gsa and Foxf1 in the intestine of CIP patients, so smooth muscle dysfunction resulting from Gsa deficiency might contribute to the development of this disease in humans.

In conclusion, we have shown that Gsa deficiency greatly decreases the contractility of intestinal smooth muscle. Gsa regulates the levels of smooth-muscle contractile proteins through CREB1-mediated Foxf1 expression, so it is crucial for normal intestinal smooth muscle contractility and functions. Mutations in the GNAS gene or altered Gsa levels may play an important role in the development of smooth muscle myopathies such as CIP.

References

1. Owens GK, Kumar MS, Wamhoff BR. Molecular regulation of vascular smooth muscle cell differentiation in development and disease. Physiol Rev 2004;84:767-801.

2. Owens GK. Molecular control of vascular smooth muscle cell differentiation and phenotypic plasticity. Novartis Found Symp 2007;283:174–191.

3. Angstenberger M, Wegener J, Pichler B, et al. Severe Intestinal Obstruction on Induced Smooth Muscle–Specific Ablation of the Transcription Factor SRF in Adult Mice. Gastroenterology 2007;133:1948–1959.

4. Mericskay M, Blanc J, Tritsch E, et al. Inducible Mouse Model of Chronic Intestinal Pseudo-Obstruction by Smooth Muscle-Specific Inactivation of the SRF Gene. Gastroenterology 2007;133:1960–1970.

5. Hoggatt AM, Kim JR, Ustiyan V, et al. The transcription factor Foxf1 binds to serum response factor and myocardin to regulate gene transcription invisceral smooth muscle cells. J Biol Chem 2013;288:28477-28487.

6. **Lei R, Zhang K**, Wei Y, et al. G-Protein α-Subunit Gsα Is Required for Craniofacial Morphogenesis. PLoS One 2016;11:e0147535.

7. Tasken K. Localized effects of cAMP mediated by distinct routes of protein kinase A. Physiol Rev 2004;84:137–167.

8. **Lu C, Xia J**, Zhou Y, et al. Loss of Gsα impairs liver regeneration through a defect in the crosstalk between cAMP and growth factor signaling. J Hepatol 2016;64:342-351.

9. Chen M, Chen H, Nguyen A, et al. Gsα deficiency in adipose tissue leads to a

lean phenotype with divergent effects on cold tolerance and diet-induced thermogenesis. Cell Metab 2010;11:320–330.

10. Sakamoto A, Chen M, Kobayashi T, et al. Chondrocyte-specific knockout of the G protein G(s)alpha leads to epiphyseal and growth plate abnormalities and ectopic chondrocyte formation. J Bone Miner Res 2005;20:663–671.

11. Patten J, Johns DR, Valle D, et al. Mutation in the gene encoding the stimulatory G protein of adenylate cyclase in Albright's hereditary osteodystrophy. N Engl J Med 1990;322:1412–1419.

12. Shenker A, Weinstein LS, Moran A, et al. Severe endocrine and nonendocrine manifestations of the McCune-Albright syndrome associated with activating mutations of stimulatory G protein GS. J Pediatr 1993;123:509–518.

13. Connor FL, Di Lorenzo C. Chronic intestinal pseudo-obstruction: assessment and management. Gastroenterology 2006;130: S29–S36.

14. Chen M, Gavrilova O, Liu J, et al. Alternative Gnas gene products have opposite effects on glucose and lipid metabolism. Proc Natl Acad Sci USA 2005;102:7386-7391.

15. **Wu Z, Yang L**, Cai L, et al. Detection of epithelial to mesenchymal transition in airways of a bleomycin induced pulmonary fibrosis model derived from an alpha-smooth muscle actin-Cre transgenic mouse. Respir Res 2007;8:1.

16. Kühbandner S, Brummer S, Metzger D, et al. Temporally controlled somatic mutagenesis in smooth muscle. Genesis 2000;28:15–22.

17. **He WQ, Peng YJ, Zhang WC**, et al. Myosin light chain kinase is central to

smooth muscle contraction and required for gastrointestinal motility in mice. Gastroenterology 2008;135:610-620.

18. van der Zee R, Welling GW. A simple method to determine the transit time in mice. Z Versuchstierkd 1983;25:233–237.

19. Miano J. Serum response factor: toggling between disparate programs of gene expression. J Mol Cell Cardiol 2003;35:577–593.

20. Knowles C, Silk DB, Darzi A, et al. Deranged smooth muscle α-actin as a biomarker of intestinal pseudo-obstruction: a controlled multinational case series. Gut 2004;53:1583-1589.

21. Wedel T, van Eys GJ, Waltregny D, et al. Novel smooth muscle markers reveal abnormalities of the intestinal musculature in severe colorectal motility disorders. Neurogastroenterol Motil 2006;18:526–538.

22. Murthy K. Signaling for contraction and relaxation in smooth muscle of the gut. Annu Rev Physiol 2006;68:345-74.

23. Connor F, Lorenzo CD. Chronic intestinal pseudo-obstruction: assessment and management. Gastroenterology 2006;130:S29–S36.

24. Hyman P, Bursch B, Sood M, et al. Visceral pain-associated disability syndrome: a descriptive analysis. J Pediatr Gastroenterol Nutr 2002;35:663–668.

Figure legends

Figure 1. **Smooth-muscle deficiency in the alpha subunit of heterotrimeric G protein (Gsa) results in postnatal lethality**. **A**, Schematic diagram of transgenic mice used to generate Gsa^{SMKO} mice. **B**, Immunohistochemistry of Cre and ACTA2 in cross sections of jejunum and ileum from Acta2-Cre mice. Scale bar = 50 µm. **C**, Western blot analysis of Gsa protein level in the jejunum, ileum and aorta from Gsa^{SMKO} mice. **D**, Western blot analysis of Gsa in the brain, skeletal muscle and skin from control and Gsa^{SMKO} mice. **E**, A typical growth curve for male mice from postnatal days 7–28 (n=6). * $p < 0.05$ *vs* control. **F**, Kaplan-Meier survival plot of control and Gsa^{SMKO} mice (n=11). * $p < 0.05$ *vs* control.

Figure 2. Impaired contraction in Gsa^{SMKO} smooth muscles. A, Representative spontaneous contractions in jejunal segments from control and Gsa^{SMKO} mice and contraction amplitudes (n=5). * $p < 0.05$ *vs* control. **B**, Transverse sections of jejunum and ileum from control and Gsa^{SMKO} mice stained with hematoxylin and eosin. Scale bar = 50 µm. **C** and **D**, Representative recordings of contraction in jejunum (**C**) and ileum (**D**) from control and Gsa^{SMKO} mice with 87 mM KCl or 1 µM acetylcholine (ACh). Bars show duration of stimulation. Shows quantification of contraction responses to KCl and ACh for jejunum and ileum (n=5). * $p < 0.05$ *vs* control. **E**, Representative recordings of contraction in jejunum from control and Gsa^{SMKO} mice with EFS. Shows quantification of contraction responses to EFS (n=5). * $p < 0.05$ *vs* control.

Figure 3. Smooth muscle-specific Gsa knockout (KO) in adult mice confers

severe intestinal obstruction. A, Schematic diagram of transgenic mice used to generate adult Gsa^{SMKO} mice induced by tamoxifen injection. **B**, A typical growth curve for male control and adult Gsa^{SMKO} mice after tamoxifen injection (n=8). * $p < 0.05$ *vs* control. **C**, Kaplan-Meier survival plot of control and adult Gsa^{SMKO} mice after tamoxifen injection (n=17). * $p < 0.05$ *vs* control. **D**, Food intake and feces excretion after 4 weeks of tamoxifen injection (n=5 each group). **E**, Gastrointestinal tract of control and adult Gsa^{SMKO} mice. Note the dilated ileum in the adult Gsa^{SMKO} mouse. **F**, Whole-gut transit time for control and adult Gsa^{SMKO} mice (n=5). * $p < 0.05$ *vs* control.

Figure 4. Gsa deletion in adult smooth muscle impairs contractility. A and **B,** Transverse sections of jejunum (**A**) and ileum (**B**) from control and adult Gsa^{SMKO} mice stained with hematoxylin and eosin. The structure of jejunum and ileum from adult Gsa^{SMKO} mice shows the hypertrophic smooth muscle layer. Scale bars for **A** and **B**: upper row, 200 µm; lower row, 50 µm. **C** and **D**, Representative recordings of jejunum (**C**) and ileum (**D**) from control and adult Gsa^{SMKO} mice with 87 mM KCl or 1 µM ACh. Shows quantification of contraction responses to KCl and ACh for jejunum and ileum (n=5). * $p < 0.05$ *vs* control. **E**, Representative recordings of contraction in jejunum from control and adult Gsa^{SMKO} mice with EFS. Shows quantification of contraction responses to EFS (n=5). * $p < 0.05$ *vs* control.

Figure 5. Gsa deletion reduced the expression of contractile proteins and cAMP/cAMP response element binding protein 1 (CREB1) signaling. A. Microarray assay of genes with >2.0-fold upregulation or >2.0-fold downregulation in

Gsa-deficient intestinal smooth muscle compared with control. **B.** Gene ontology enrichment analysis of differentially expressed genes. The number of genes with a significantly changed expression is shown in parentheses. **C.** Top 10 enrichment pathways based on the KEGG database. **D.** Quantitative RT-PCR of genes related to smooth muscle contraction for validation of the microarray results (n=5). * $p < 0.05$ *vs* control. **E,** The jejunum tissue from control and adult Gsa^{SMKO} mice was stimulated with 10 μM ISO for 5 minutes followed by cAMP measurement and western blot to detect the levels of p-CREB1 and total CREB1. n=5, * $p < 0.05$ *vs* control. **F**, Western blot analysis of protein levels of p-CREB1, total CREB1 and Foxf1 in muscle tissue from control and adult Gsa^{SMKO} mice.

Figure 6. CREB1 binds with Foxf1 promoter and regulates its expression. A, Predicted CRE site in the mouse Foxf1 promoter. **B,** Mouse intestinal SMCs were treated with 10 μM forskolin for 24 hours and western blot was used to detect Foxf1 expression. The levels of Foxf1 were quantified (n=4). *$p<0.05$ *vs* 0h. **C**, Mouse intestinal SMCs were treated with 10 μM forskolin for 12 hr, ChIP was then used to assy the CREB1 binding site in the Foxf1 promoter. **D**, Mouse intestinal SMCs were transfected with WT or mutant Foxf1 promoter luciferase constructs, then treated with forskolin for 24 hr and luciferase activity was measured. Results of the luciferase promoter assay are presented as fold change ± SEM of firefly/Renilla luciferase activity (n=4). * $p < 0.05$ vs WT-luc + Mock.

Figure 7. Levels of Gsa, Foxf1 and p-CREB1/CREB1 were reduced in the intestinal muscle layer of CIP patients. A, Paraffin-embedded control and CIP

specimens from patients were stained with primary antibodies for Gsa, Foxf1, p-CREB1 and total CREB1, then secondary antibody HRP-DAB (3,3'-diaminobenzidine) detection reagents (brown). Scale bar: 50 μm. **B**, Quantification of Gsa, Foxf1, p-CREB1 and total CREB1 levels by normalization to DAB intensity in control specimens (set to 1) (n=5). *p<0.05 *vs* control. **C**, Diagram for Gsa-regulated intestinal smooth-muscle function via CREB1/Foxf1. AC, adenylyl cyclase.

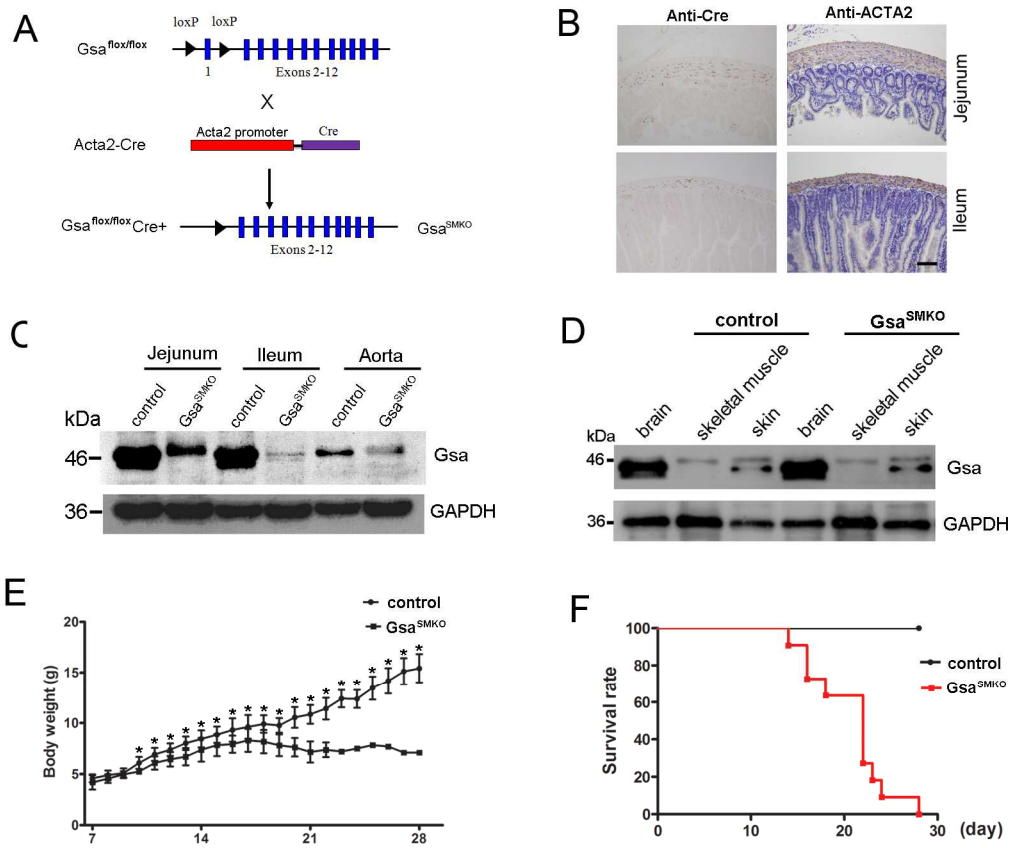

Figure 1. **Smooth-muscle deficiency in the alpha subunit of heterotrimeric G protein (Gsa) results in postnatal lethality**. **A**, Schematic diagram of transgenic mice used to generate Gsa^{SMKO} mice. **B**, Immunohistochemistry of Cre and ACTA2 in cross sections of jejunum and ileum from Acta2-Cre mice. Scale bar = 50 μm. **C**, Western blot analysis of Gsa protein level in the jejunum, ileum and aorta from Gsa^{SMKO} mice. **D**, Western blot analysis of Gsa in the brain, skeletal muscle and skin from control and Gsa^{SMKO} mice. **E**, A typical growth curve for male mice from postnatal days 7–28 (n=6). * $p < 0.05$ *vs* control. **F**, Kaplan-Meier survival plot of control and Gsa^{SMKO} mice (n=11). * $p < 0.05$ *vs* control.

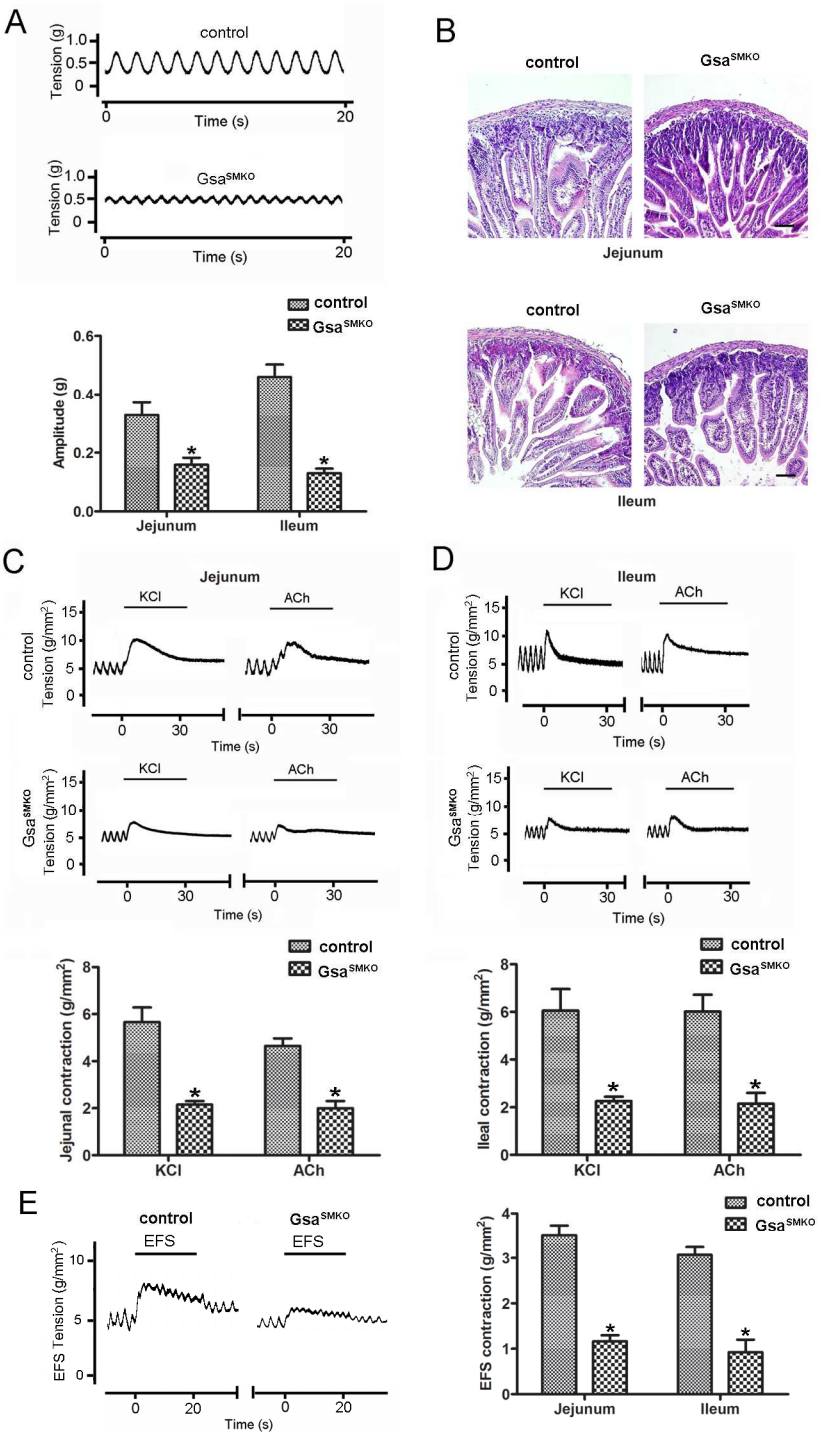

Figure 2. Impaired contraction in Gsa^{SMKO} smooth muscles. A, Representative spontaneous contractions in jejunal segments from control and Gsa^{SMKO} mice and contraction amplitudes (n=5). * $p < 0.05$ *vs* control. **B**, Transverse sections of jejunum and ileum from control and Gsa^{SMKO} mice stained with hematoxylin and eosin. Scale bar = 50 µm. **C** and **D**, Representative recordings of contraction in jejunum (**C**) and ileum (**D**) from control and Gsa^{SMKO} mice with 87 mM KCl or 1 µM acetylcholine (ACh). Bars show duration of stimulation. Shows quantification of contraction responses to KCl and ACh for jejunum and ileum (n=5). * $p < 0.05$ *vs* control. **E**, Representative recordings of contraction in jejunum from control and Gsa^{SMKO} mice with EFS. Shows quantification of contraction responses to EFS (n=5). * $p < 0.05$ *vs* control.

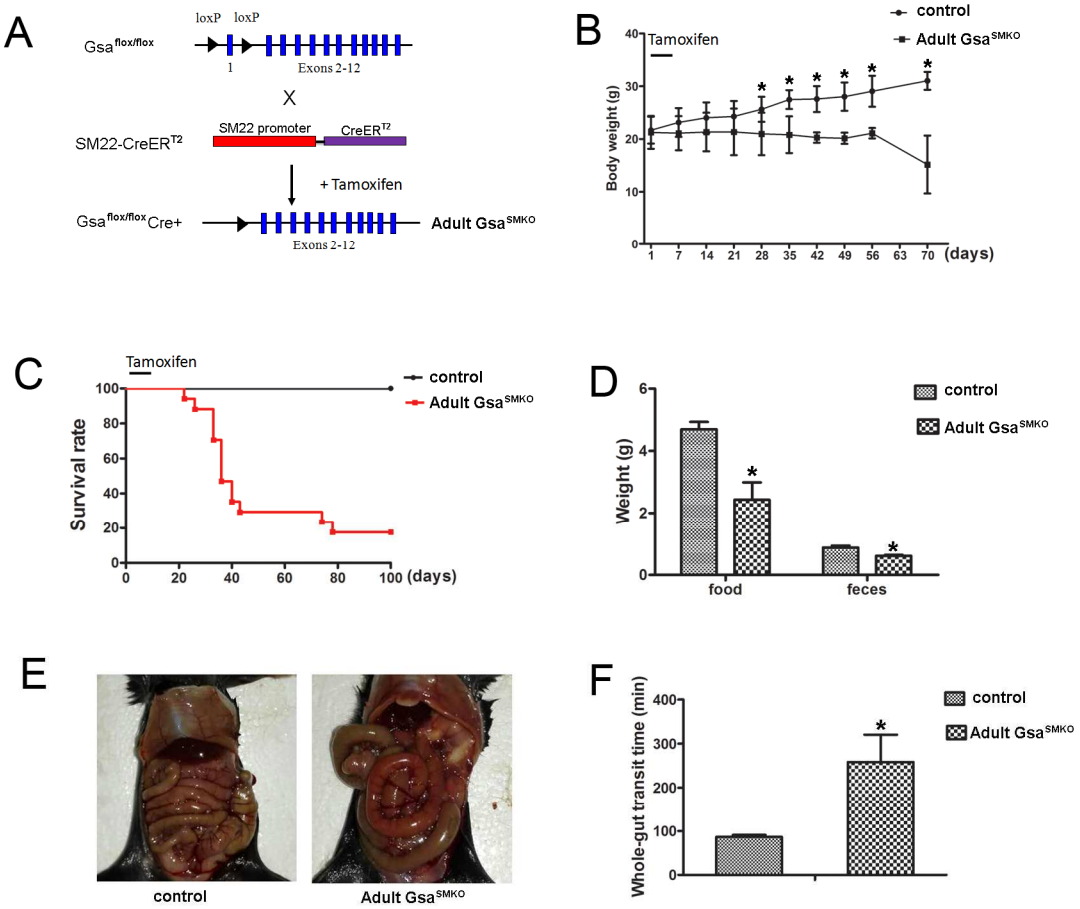

Figure 3. Smooth muscle-specific Gsa knockout (KO) in adult mice confers severe intestinal obstruction. A, Schematic diagram of transgenic mice used to generate adult Gsa^{SMKO} mice induced by tamoxifen injection. **B**, A typical growth curve for male control and adult Gsa^{SMKO} mice after tamoxifen injection (n=8). * $p < 0.05$ *vs* control. **C**, Kaplan-Meier survival plot of control and adult Gsa^{SMKO} mice after tamoxifen injection (n=17). * $p < 0.05$ *vs* control. **D**, Food intake and feces excretion after 4 weeks of tamoxifen injection (n=5 each group). **E**, Gastrointestinal tract of control and adult Gsa^{SMKO} mice. Note the dilated ileum in the adult Gsa^{SMKO} mouse. **F**, Whole-gut transit time for control and adult Gsa^{SMKO} mice (n=5). * $p < 0.05$ *vs* control.

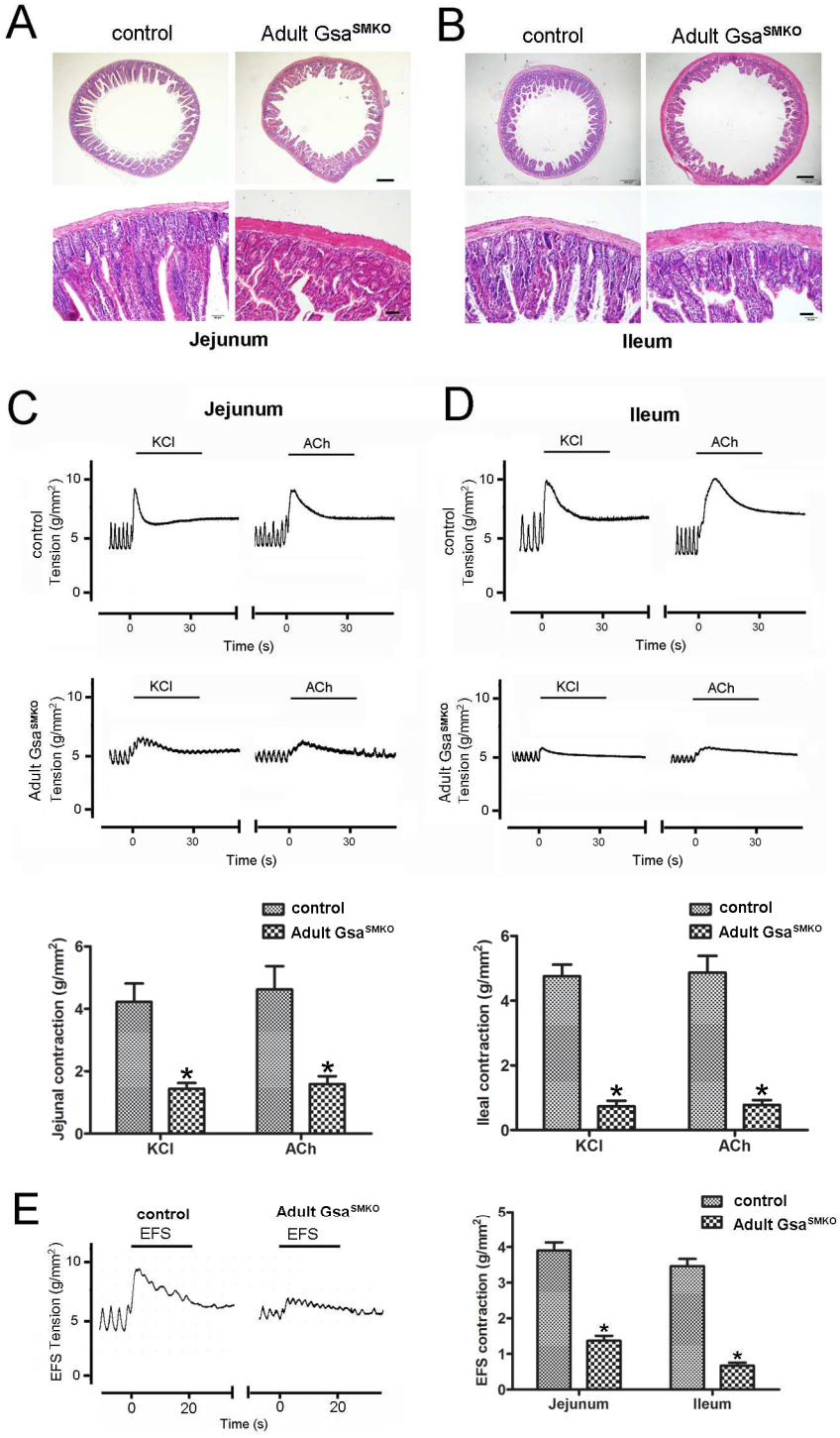

Figure 4. Gsa deletion in adult smooth muscle impairs contractility. A and **B,** Transverse sections of jejunum (**A**) and ileum (**B**) from control and adult Gsa^{SMKO} mice stained with hematoxylin and eosin. The structure of jejunum and ileum from adult Gsa^{SMKO} mice shows the hypertrophic smooth muscle layer. Scale bars for **A** and **B**: upper row, 200 µm; lower row, 50 µm. **C** and **D**, Representative recordings of jejunum (**C**) and ileum (**D**) from control and adult Gsa^{SMKO} mice with 87 mM KCl or 1 µM ACh. Shows quantification of contraction responses to KCl and ACh for jejunum and ileum (n=5). * $p < 0.05$ *vs* control. **E**, Representative recordings of contraction in jejunum from control and adult Gsa^{SMKO} mice with EFS. Shows quantification of contraction responses to EFS (n=5). * $p < 0.05$ *vs* control.

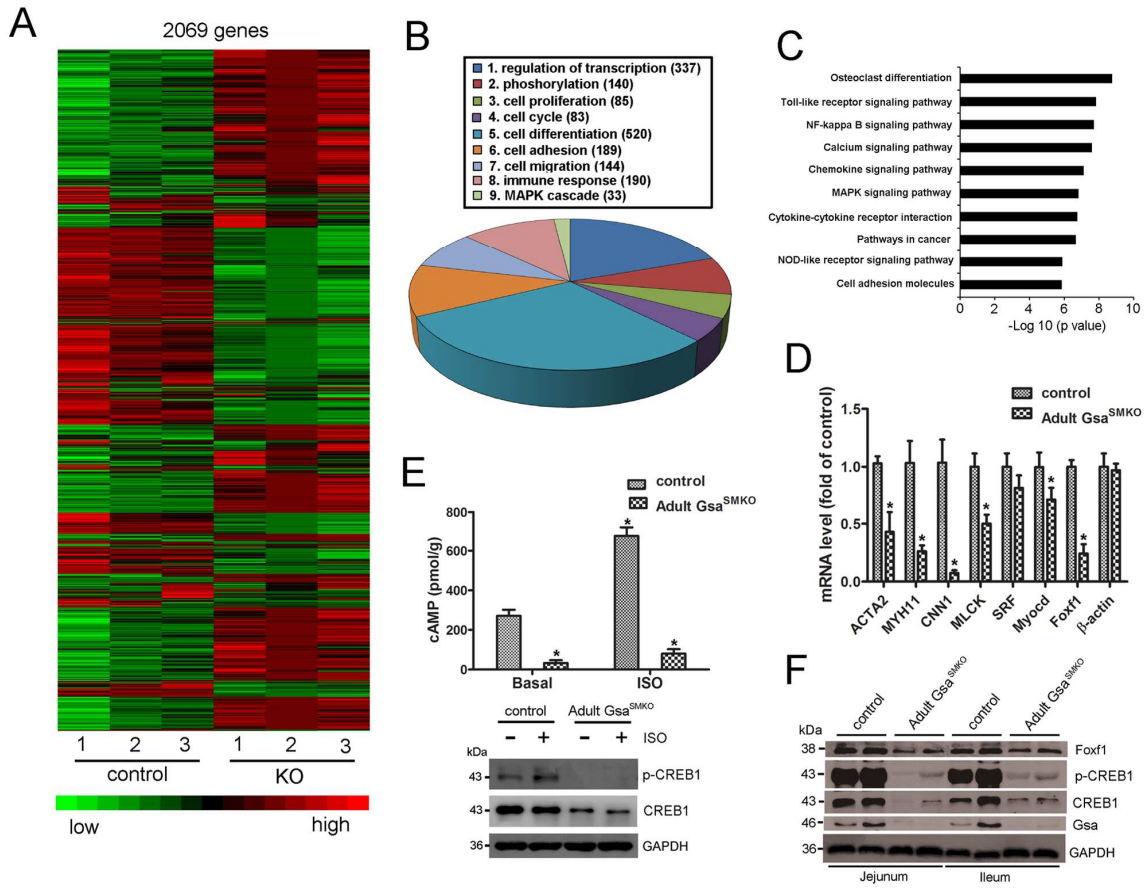

Figure 5. Gsa deletion reduced the expression of contractile proteins and cAMP/cAMP response element binding protein 1 (CREB1) signaling. A. Microarray assay of genes with >2.0-fold upregulation or >2.0-fold downregulation in Gsa-deficient intestinal smooth muscle compared with control. **B.** Gene ontology enrichment analysis of differentially expressed genes. The number of genes with a significantly changed expression is shown in parentheses. **C.** Top 10 enrichment pathways based on the KEGG database. **D.** Quantitative RT-PCR of genes related to smooth muscle contraction for validation of the microarray results (n=5). * $p < 0.05$ *vs* control. **E**, The jejunum tissue from control and adult Gsa^{SMKO} mice was stimulated with 10 μM ISO for 5 minutes followed by cAMP measurement and western blot to detect the levels of p-CREB1 and total CREB1. n=5, * $p < 0.05$ *vs* control. **F**, Western blot analysis of protein levels of p-CREB1, total CREB1 and Foxf1 in muscle tissue from control and adult Gsa^{SMKO} mice.

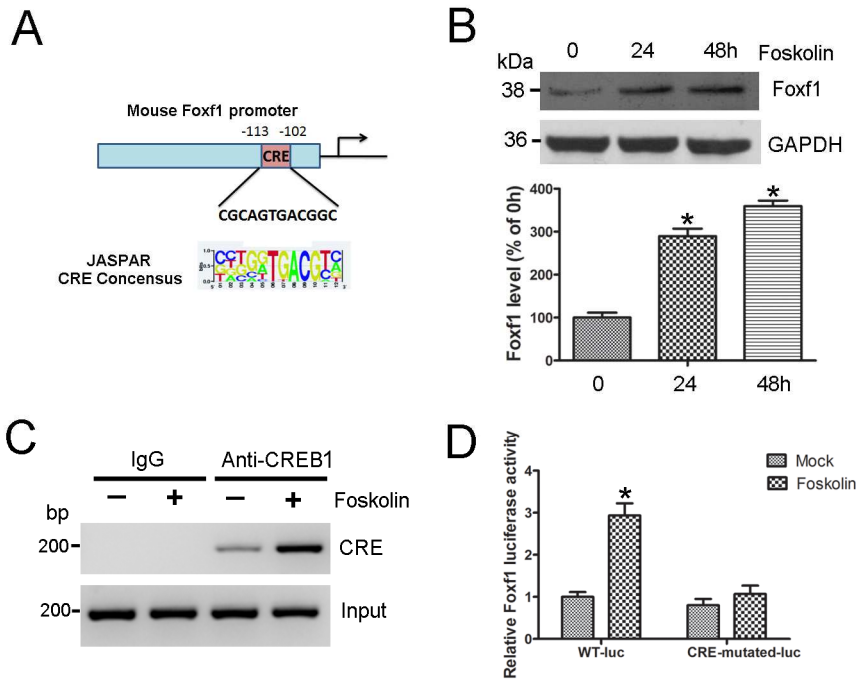

Figure 6. CREB1 binds with Foxf1 promoter and regulates its expression. A, Predicted CRE site in the mouse Foxf1 promoter. **B,** Mouse intestinal SMCs were treated with 10 μM forskolin for 24 hours and western blot was used to detect Foxf1 expression. The levels of Foxf1 were quantified (n=4). *p<0.05 *vs* 0h. **C**, Mouse intestinal SMCs were treated with 10 μM forskolin for 12 hr, ChIP was then used to assy the CREB1 binding site in the Foxf1 promoter. **D**, Mouse intestinal SMCs were transfected with WT or mutant Foxf1 promoter luciferase constructs, then treated with forskolin for 24 hr and luciferase activity was measured. Results of the luciferase promoter assay are presented as fold change ± SEM of firefly/Renilla luciferase activity (n=4). * p < 0.05 vs WT-luc + Mock.

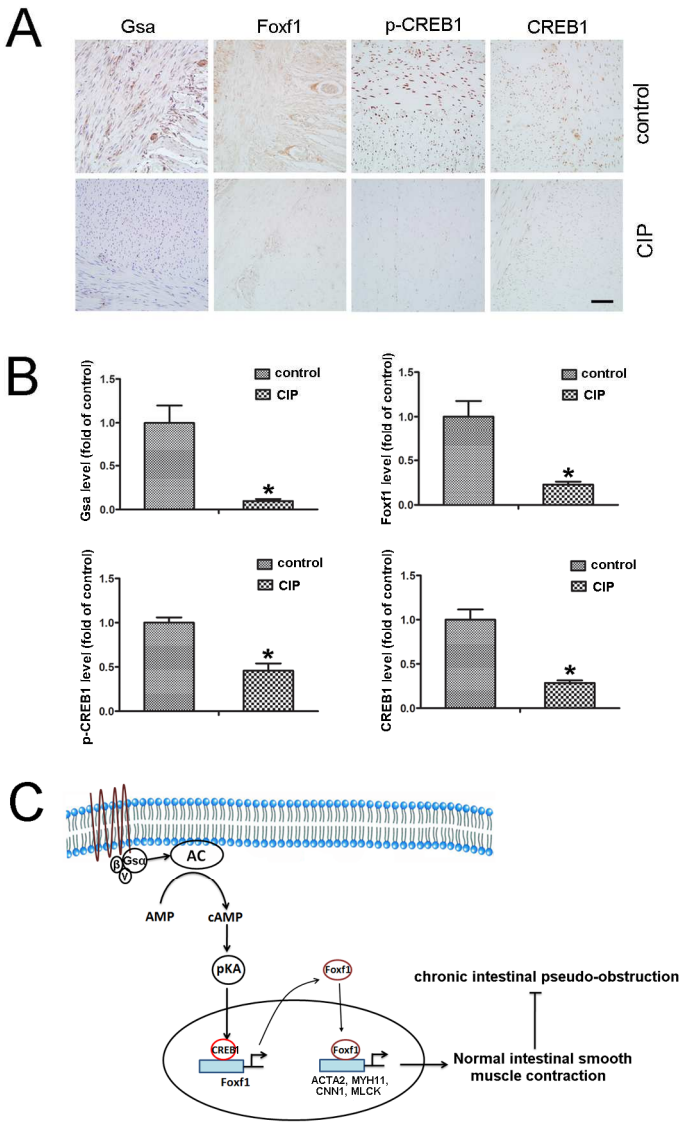

Figure 7. Levels of Gsa, Foxf1 and p-CREB1/CREB1 were reduced in the intestinal muscle layer of CIP patients. A, Paraffin-embedded control and CIP specimens from patients were stained with primary antibodies for Gsa, Foxf1, p-CREB1 and total CREB1, then secondary antibody HRP-DAB (3,3'-diaminobenzidine) detection reagents (brown). Scale bar: 50 μm. **B**, Quantification of Gsa, Foxf1, p-CREB1 and total CREB1 levels by normalization to DAB intensity in control specimens (set to 1) (n=5). *p<0.05 *vs* control. **C**, Diagram for Gsa-regulated intestinal smooth-muscle function via CREB1/Foxf1. AC, adenylyl cyclase.

Supplement

Heterotrimeric G Stimulatory Protein alpha subunit is Required for Intestinal Smooth Muscle Contraction in Mice

Xiaoteng Qin[1], Shangming Liu[1,2], Qiulun Lu[3], Meng Zhang[1], Xiuxin Jiang[4], Sanyuan Hu[4], Jingxin Li[5], Cheng Zhang[1], Jiangang Gao[6], Min-Sheng Zhu[7], Yun Zhang[1*] and Wencheng Zhang[1*]

Supplementary Materials and Methods

Chemicals and Antibodies

Acetylcholine (ACh), isoprenaline and forskolin were from Sigma (St Louis, MO). cAMP measurement kit was from ENZO Life Sciences (Loerrach, Germany). Antibodies used in this study were specific for Gsa (ab83735, Abcam, Cambridge, UK), Foxf1 (AV32296, Sigma), phospho-CREB1 S133 (9198, Cell Signaling, Danvers, MA), total CREB1 (9197, Cell Signaling), ACTA2 (ab5694, Abcam), MYH11 (21404-1-AP, Proteintech), CNN1 (13938-1-AP, Proteintech), MLCK (21642-1-AP, Proteintech), ADRB1 (ab3442, Abcam), ADRB2 (13096-1-AP, Proteintech), β-actin (60008-1-Ig, Proteintech) and GAPDH (10494-1-AP, Proteintech).

Histology

Fresh gut tissues were fixed by incubation in 4% formalin, embedded in paraffin, and sectioned transversely at 5 μm thick. For staining preparation, the slides were

dewaxed with xylene, rehydrated with descending grades of ethanol, then rinsed with distilled water. Tissue sections were stained with hematoxylin and eosin to examine the morphology of the intestine.

SDS-PAGE and Western blot

Protein extracts were prepared by lysing tissues or cells in RIPA lysis buffer from Santa Cruz Biotechnology. Cleared lysates were separated on 10% Tris-glycine gels followed by transfer onto nitrocellulose membranes. After blocking in 5% skim milk, blots were probed using specific antibodies. The intensities of individual bands were measured by densitometry (Model GS-700, Imaging Densitometer; Bio-Rad, Hercules, CA).

Quantitative Real-time PCR

Total RNA was extracted from frozen tissues (kept at -80°C) by using Tri Reagent (Ambion, Austin, TX), and 1 μg of RNA was reverse-transcribed into cDNA by using iScriptcDNA Synthesis Kits (Bio-Rad, Hercules, CA). PCR amplification involved the SYBR PCR mix (Bio-Rad). The oligonucleotide primer sequences used were for MYH11, 5'-GAGGTGGTCGTGGAGTTGGT-3' and 5'-GTATCGCTCCCTCAGGTTGT-3'; ACTA2, 5'-GAGAAGCCCAGCCAGTCG-3' and 5'-CTCTTGCTCTGGGCTTCA-3'; CNN1, 5'-CACCAACAAGTTTGCCAG-3' and 5'-TGTGTCGCAGTGTTCCAT-3'; MLCK, 5'-ACATGCTACTGAGTGGCCTCTCT-3' and 5'-GGCAGACAGGACATTGTTTAAGG-3'; Foxf1,

5'-CATACCTTCACCAAAACAGTCACAA-3' and 5'-AAACTCTCTGTCACACATGCT-3'; SRF: 5'-GTTCATCGACAACAAGCTGC-3' and 5'-CTGTCAGCGTGGACAGCTCATAG-3'; Myocd: 5'-CAGCTACCCTGGGATGCACCAAACAC-3' and 5'-GGGGCCTGGTTTGAGAGAAGAAACACC-3'; GAPDH, 5'-TTGTCAAGCTCATTTCCTGGTATG-3' and 5'-GCCATGTAGGCCATGAGGTC-3'.

Primary Culture of Intestinal SMCs

Mouse intestinal SMCs were cultured as described before [1]. Briefly, eight- to 12-week-old mice were killed by cervical dislocation. Segments of the jejunum were excised and washed at least three times in ice-cold Hanks' solution (137.93 mM NaCl, 5.33 mM KCl, 4.17 mM $NaHCO_3$, 0.441 mM KH_2PO_4, 0.338 mM Na_2HPO_4, 5.56 mM D-glucose, 500 units/ml penicillin, and 500 μg/ml streptomycin). The mesentery and related tissues were removed. Muscularis propria were carefully teased away from the remaining intestine segments with micro-tweezers. Then, the muscle layers were minced into fragments (less than 1 cubic millimeter) in DMEM containing 20% (v/v) fetal bovine serum (FBS), L-glutamine, non-essential amino acids (NEAA) (Invitrogen), 100 units/ml penicillin and 100 μg/ml streptomycin. The suspension was transferred to culture dishes coated with 0.1% gelatin (Sigma-Aldrich) and then incubated at 37 °C in a humidified atmosphere of 5% CO_2. The intestinal SMCs started to migrate from the explants after 4 to 6 days. Finally, the cell monolayer was

passaged after 10 to 12 days and cultured in DMEM containing 10% (v/v) FBS, L-glutamine, NEAA, 100 units/ml penicillin, and 100 μg/ml streptomycin.

Chromatin Immunoprecipitation (ChIP) Assay

ChIP analyses of SMCs involved the Magna ChIP A/G Chromatin Immunoprecipitation Kit (Millipore, Temecula, CA). Mouse intestinal SMCs were treated with or without 10 μM forskolin for 12 hr, then cross-linked by using formaldehyde; DNA was sheared by sonication and incubated with 1 μg normal rabbit IgG or anti-CREB1 antibody. Immunoprecipitation was performed with the magnetic beads included in the kit. For PCR, 2 μl of the 50-μl total immunoprecipitated DNA was analyzed with the following primer sequences: CRE, 5'-CTGATGCGCGTGGCCTCCCG-3' and 5'-GCTGCCGAGCCGGGAGGAGG-3'.

DNA constructs and luciferase reporter assays

The DNA fragment from the mouse Foxf1 promoter cloned into pGL3Basic (Promega, Madison, WI) to generate the wild-type (WT)-luc construct was amplified by PCR with the primer sequences 5'-GGTACCGCTCTGTGAATTCAGATCTG-3' and 5'-AAGCTTCCGCCGCCGCTGCCGCCGCT-3'. Mutant constructs of the predicted CRE sites in the Foxf1 promoter were generated by site-directed mutagenesis (Promega) with the primer sequences 5'-GGCGGCTGCACCTCTGCTACTGCTGCGGCTCCCGAGCGC-3' and 5'-GCGCTCGGGAGCCGCAGCAGTAGCAGAGGTGCAGCCGCC-3'. For luciferase assay, the luciferase reporter plasmid was transfected into intestinal SMCs

in 24-well plates by using FuGene HD reagent (Roche Applied Science, Indianapolis, IN). The pRL-TK plasmid carrying the Renilla luciferase under the control of the thymidine kinase promoter was co-transfected as an internal control for transfection efficiency. Cells were treated with 10 μM forskolin for 24 hr and luciferase activities were analyzed by using the Dual-Luciferase Assay Kit (Promega).

Microarray analysis

Total RNA was extracted from control and Gsa-deficient intestinal smooth muscle. For human cases, total RNA was extracted from ileal smooth muscle of patients with CIP and age-matched control. The transcriptome sequencing experiments were performed for microarray assay by Vazyme Biotech (Nanjing, China). The transcriptome library for sequencing was generated using VAHTS™ mRNA-seq v2 Library Prep Kit for Illumina® (Vazyme Biotech Co., Ltd, Nanjing, China) following the manufacturer's recommendations. The clustering of the index-coded samples was used VAHTS RNA Adapters set1/set2 for Illumina® (Vazyme Biotech Co., Ltd, Nanjing, China). After clustering, the libraries were sequenced on Illumina Hiseq X Ten platform using (2×150 bp) paired-end module. The differentially expressed genes were identified with q value ≤0.05 and a fold-change of ≥2 between two samples. Cluster analysis, Gene Ontology (GO) enrichment analysis and Pathway enrichment analysis of differentially expressed genes were performed.

References

1. Chen C, Tao T, Wen C, He WQ, Qiao YN, Gao YQ, Chen X, Wang P, Chen CP, Zhao W, Chen HQ, Ye AP, Peng YJ, Zhu MS. Myosin light chain kinase (MLCK) regulates cell migration in a myosin regulatory light chain phosphorylation-independent mechanism. *J Biol Chem*. 2014; **289**:28478-88.

Figure legends

Supplementary Figure 1. Acta2-Cre or SM22-CreER^{T2} mediated Gsa knockout happened in smooth muscle layer. A-C, Immunohistochemistry of Gsa and ACTA2 in cross sections of aorta (**A**), jejunum (**B**) and ileum (**C**) from control and Gsa^{SMKO} mice. Scale bars in panel A represent 500 μm; scale bars in panel B and C represent 50 μm. **D-E**, Immunohistochemistry of Gsa and ACTA2 in cross sections of jejunum (**D**) and ileum (**E**) from control and adult Gsa^{SMKO} mice. Scale bars in panel D and E represent 50 μm.

Supplementary Figure 2. Gsa knockout in smooth muscle impaired contraction. A and **B**, The jejunum (**A**) and ileum (**B**) from control and Gsa^{SMKO} mice at 13 days was treated with 87 mM KCl, 1 μM ACh or electrical field stimulation (EFS) (20 Hz, 30 V, pulse train, 20 s) followed by quantitative analysis (n=5). * $p < 0.05$ *vs* control.

Supplementary Figure 3. Gsa deletion in smooth muscle reduced the expression of contractile proteins. A, Western blot analysis of the levels of contractile proteins from control and adult Gsa^{SMKO} mice. **B**, Quantitative analysis of the levels of contractile proteins from control and adult Gsa^{SMKO} mice (n=4). * $p < 0.05$ *vs* control.

Supplementary Figure 4. Microarray analysis of gene expression from human and mice tissues. A, Microarray assay of genes with >2.0-fold upregulation or >2.0-fold downregulation in patients with CIP compared with age-matched control group. **B**, Top 9 enrichment pathways with a significantly changed genes based on the KEGG database. **C**, Venn diagram of differentially expressed genes in patients with

CIP compared to control and Gsa KO compared to control found in microarray analysis (>2-fold). **D**, A list of common genes with over 2-fold upregulation both in the groups of patients with CIP and Gsa KO. **E**, A list of common genes with over 2-fold downregulation both in the groups of patients with CIP and Gsa KO.

Supplementary Table 1. Detailed list of differentially expressed genes with over 2-fold upregulation or over 2-fold downregulation in Gsa-deficient intestinal smooth muscle.

Supplementary Table 2. Detailed list of differentially expressed genes with over 2-fold upregulation or over 2-fold downregulation in the intestinal smooth muscle from patients with CIP.

GeneID	GeneName	GenePos	WT_FPKM	KO_FPKM	log2(KO/W	up-or-d	p_value	q_value	Description
ENSMUSG(	6330408A0	7:1325896	142.627	1.79703	-6.31048	down	5.00E-05	0.001113	RIKEN cDNA 6330408A02 gene [Source:MGI Symbol;Acc:MGI:24478
ENSMUSG(	Gnas	2:1742812	5.80328	0.073923	-6.2947	down	0.00105	0.012218	GNAS (guanine nucleotide binding protein, alpha stimulating) comp
ENSMUSG(	Phactr1	13:426806	168.422	5.25376	-5.00258	down	5.00E-05	0.001113	phosphatase and actin regulator 1 [Source:MGI Symbol;Acc:MGI:26
ENSMUSG(	Ntrk3	7:7817595	16.6072	0.553942	-4.90593	down	5.00E-05	0.001113	neurotrophic tyrosine kinase, receptor, type 3 [Source:MGI Symbol;
ENSMUSG(	Khdrbs2	1:3217271	9.75729	0.388685	-4.64981	down	0.0001	0.001959	KH domain containing, RNA binding, signal transduction associated
ENSMUSG(	Dclk3	9:1114390	0.963183	0.040162	-4.5839	down	0.0042	0.034371	doublecortin-like kinase 3 [Source:MGI Symbol;Acc:MGI:3039580]
ENSMUSG(	Fam198a	9:1219509	2.07891	0.111603	-4.21938	down	0.0001	0.001959	family with sequence similarity 198, member A [Source:MGI Symbo
ENSMUSG(	Col9a2	4:1210393	4.11825	0.2384	-4.11057	down	5.00E-05	0.001113	collagen, type IX, alpha 2 [Source:MGI Symbol;Acc:MGI:88466]
ENSMUSG(	Hs3st5	10:365068	0.929031	0.057009	-4.02647	down	0.0019	0.018936	heparan sulfate (glucosamine) 3-O-sulfotransferase 5 [Source:MGI S
ENSMUSG(	Anpep	7:7982180	81.2663	5.0101	-4.01975	down	5.00E-05	0.001113	alanyl (membrane) aminopeptidase [Source:MGI Symbol;Acc:MGI:5
ENSMUSG(	Scn9a	2:6644087	0.84875	0.05394	-3.97592	down	5.00E-05	0.001113	sodium channel, voltage-gated, type IX, alpha [Source:MGI Symbol;
ENSMUSG(	Iqsec3	6:1213729	0.757907	0.048498	-3.96603	down	5.00E-05	0.001113	IQ motif and Sec7 domain 3 [Source:MGI Symbol;Acc:MGI:2677208
ENSMUSG(	Stac	9:1115614	3.37471	0.231285	-3.86702	down	0.00155	0.016271	src homology three (SH3) and cysteine rich domain [Source:MGI Syr
ENSMUSG(	Nalcn	14:123276	0.801857	0.056098	-3.83733	down	0.00585	0.043923	sodium leak channel, non-selective [Source:MGI Symbol;Acc:MGI:24
ENSMUSG(	Scn11a	9:1197537	1.06938	0.075525	-3.82368	down	0.00055	0.007646	sodium channel, voltage-gated, type XI, alpha [Source:MGI Symbol;
ENSMUSG(	Fmod	1:1340372	40.6944	2.88955	-3.81591	down	5.00E-05	0.001113	fibromodulin [Source:MGI Symbol;Acc:MGI:1328364]
ENSMUSG(	Kcnj5	9:3231478	0.866035	0.063852	-3.76161	down	0.00195	0.019322	potassium inwardly-rectifying channel, subfamily J, member 5 [Sour
ENSMUSG(	Necab1	4:1492990	3.01025	0.225991	-3.73554	down	0.00355	0.030479	N-terminal EF-hand calcium binding protein 1 [Source:MGI Symbol;
ENSMUSG(	Unc5c	3:1414579	0.676952	0.051417	-3.71873	down	0.0005	0.007097	unc-5 homolog C (C. elegans) [Source:MGI Symbol;Acc:MGI:109541
ENSMUSG(	Gdf10	14:339235	27.7791	2.12046	-3.71155	down	5.00E-05	0.001113	growth differentiation factor 10 [Source:MGI Symbol;Acc:MGI:9568
ENSMUSG(	Cnga3	1:3721443	1.10653	0.085556	-3.69304	down	0.00035	0.005412	cyclic nucleotide gated channel alpha 3 [Source:MGI Symbol;Acc:M
ENSMUSG(	Ooep	9:7837610	1.67435	0.132987	-3.65424	down	0.0024	0.022628	oocyte expressed protein [Source:MGI Symbol;Acc:MGI:1915218]
ENSMUSG(	C1qtnf3	15:109523	30.6346	2.44586	-3.64675	down	5.00E-05	0.001113	C1q and tumor necrosis factor related protein 3 [Source:MGI Symbo
ENSMUSG(	Dbp	7:4570524	106.787	8.52862	-3.64628	down	0.00095	0.011316	D site albumin promoter binding protein [Source:MGI Symbol;Acc:M
ENSMUSG(	Esrrg	1:1876087	1.18955	0.097877	-3.60331	down	0.00015	0.002736	estrogen-related receptor gamma [Source:MGI Symbol;Acc:MGI:13
ENSMUSG(	Slc5a7	17:542735	3.57568	0.296199	-3.59358	down	5.00E-05	0.001113	solute carrier family 5 (choline transporter), member 7 [Source:MGI
ENSMUSG(	Fgf14	14:123977	0.624472	0.052224	-3.57985	down	0.00535	0.041142	fibroblast growth factor 14 [Source:MGI Symbol;Acc:MGI:109189]
ENSMUSG(	Nefl	14:680825	2.54198	0.21322	-3.57554	down	0.00375	0.031517	neurofilament, light polypeptide [Source:MGI Symbol;Acc:MGI:9731
ENSMUSG(	Nrep	18:334370	50.302	4.23602	-3.56983	down	5.00E-05	0.001113	neuronal regeneration related protein [Source:MGI Symbol;Acc:MG
ENSMUSG(	Cntnap5a	1:1156847	0.487422	0.041239	-3.56309	down	0.00035	0.005412	contactin associated protein-like 5A [Source:MGI Symbol;Acc:MGI:3
ENSMUSG(	Nlgn3	X:1012740	0.641491	0.054377	-3.56036	down	0.00475	0.037644	neuroligin 3 [Source:MGI Symbol;Acc:MGI:2444609]
ENSMUSG(	Tub	7:1089503	2.88743	0.246931	-3.54761	down	0.00225	0.021541	tubby candidate gene [Source:MGI Symbol;Acc:MGI:2651573]
ENSMUSG(	Ret	6:1181517	5.84635	0.506118	-3.52999	down	5.00E-05	0.001113	ret proto-oncogene [Source:MGI Symbol;Acc:MGI:97902]
ENSMUSG(	Nptx1	11:119538	8.46103	0.738704	-3.51777	down	5.00E-05	0.001113	neuronal pentraxin 1 [Source:MGI Symbol;Acc:MGI:107811]
ENSMUSG(	Nkx3-2	5:4176148	8.76428	0.780057	-3.48998	down	5.00E-05	0.001113	NK3 homeobox 2 [Source:MGI Symbol;Acc:MGI:108015]
ENSMUSG(	Kif26a	12:112146	0.764906	0.068262	-3.48614	down	0.00225	0.021541	kinesin family member 26A [Source:MGI Symbol;Acc:MGI:2447072]
ENSMUSG(	Nmu	5:7633123	20.5657	1.83635	-3.48533	down	5.00E-05	0.001113	neuromedin U [Source:MGI Symbol;Acc:MGI:1860476]
ENSMUSG(	Adra2a	19:540451	1.85141	0.165479	-3.4839	down	0.00035	0.005412	adrenergic receptor, alpha 2a [Source:MGI Symbol;Acc:MGI:87934]
ENSMUSG(	Pcdh20	14:884647	2.09769	0.188024	-3.47982	down	5.00E-05	0.001113	protocadherin 20 [Source:MGI Symbol;Acc:MGI:2443376]
ENSMUSG(	Cnr1	4:3392459	5.74201	0.516757	-3.474	down	5.00E-05	0.001113	cannabinoid receptor 1 (brain) [Source:MGI Symbol;Acc:MGI:10461
ENSMUSG(	Adgrb3	1:2506747	1.30519	0.117796	-3.46989	down	0.0012	0.013499	adhesion G protein-coupled receptor B3 [Source:MGI Symbol;Acc:M
ENSMUSG(	Pdzk1ip1	4:1150887	8.20355	0.742209	-3.46635	down	0.0017	0.017457	PDZK1 interacting protein 1 [Source:MGI Symbol;Acc:MGI:1914432]
ENSMUSG(	Entpd1	19:406123	114.508	10.4215	-3.45782	down	5.00E-05	0.001113	ectonucleoside triphosphate diphosphohydrolase 1 [Source:MGI Sy
ENSMUSG(	Gpr149	3:6252907	2.26304	0.208702	-3.43874	down	0.0002	0.003484	G protein-coupled receptor 149 [Source:MGI Symbol;Acc:MGI:2443
ENSMUSG(	Bche	3:7363580	18.4253	1.71456	-3.42577	down	5.00E-05	0.001113	butyrylcholinesterase [Source:MGI Symbol;Acc:MGI:894278]
ENSMUSG(	Slc7a14	3:3120285	2.22669	0.208796	-3.41473	down	5.00E-05	0.001113	solute carrier family 7 (cationic amino acid transporter, y+ system),
ENSMUSG(	Optc	1:1338971	181.334	17.1225	-3.40469	down	0.0035	0.030183	opticin [Source:MGI Symbol;Acc:MGI:2151113]
ENSMUSG(	Slc29a4	5:1426925	2.11888	0.201947	-3.39125	down	0.0012	0.013499	solute carrier family 29 (nucleoside transporters), member 4 [Sourc
ENSMUSG(	P2rx2	5:1103398	5.17823	0.497906	-3.37851	down	0.00055	0.007646	purinergic receptor P2X, ligand-gated ion channel, 2 [Source:MGI Sy
ENSMUSG(	Chgb	2:1327812	5.22285	0.505719	-3.36843	down	5.00E-05	0.001113	chromogranin B [Source:MGI Symbol;Acc:MGI:88395]
ENSMUSG(	Fat4	3:3887456	2.65218	0.259316	-3.3544	down	5.00E-05	0.001113	FAT atypical cadherin 4 [Source:MGI Symbol;Acc:MGI:3045256]
ENSMUSG(	Retnla	16:488425	24.592	2.42231	-3.34374	down	0.0001	0.001959	resistin like alpha [Source:MGI Symbol;Acc:MGI:1888504]
ENSMUSG(	Nell2	15:952194	14.9546	1.49008	-3.32713	down	5.00E-05	0.001113	NEL-like 2 [Source:MGI Symbol;Acc:MGI:1858510]
ENSMUSG(	Ndst4	3:1254040	0.99665	0.099691	-3.32155	down	0.0004	0.005949	N-deacetylase/N-sulfotransferase (heparin glucosaminyl) 4 [Source:
ENSMUSG(	Elavl3	9:2201500	1.13775	0.114602	-3.31148	down	0.0012	0.013499	ELAV (embryonic lethal, abnormal vision, Drosophila)-like 3 (Hu anti
ENSMUSG(	L1cam	X:7385377	8.58903	0.865992	-3.31007	down	0.0034	0.029484	L1 cell adhesion molecule [Source:MGI Symbol;Acc:MGI:96721]
ENSMUSG(	Dpp6	5:2681720	2.61559	0.264202	-3.30743	down	5.00E-05	0.001113	dipeptidylpeptidase 6 [Source:MGI Symbol;Acc:MGI:94921]
ENSMUSG(	Dbh	2:2716523	1.08863	0.109967	-3.30737	down	0.00645	0.047154	dopamine beta hydroxylase [Source:MGI Symbol;Acc:MGI:94864]
ENSMUSG(	Tmprss5	9:4908125	8.07192	0.816629	-3.30516	down	0.00015	0.002736	transmembrane protease, serine 5 (spinesin) [Source:MGI Symbol;A
ENSMUSG(	Postn	3:5436110	99.3268	10.1093	-3.2965	down	5.00E-05	0.001113	periostin, osteoblast specific factor [Source:MGI Symbol;Acc:MGI:19
ENSMUSG(	Ache	5:1372740	10.6125	1.0823	-3.29359	down	5.00E-05	0.001113	acetylcholinesterase [Source:MGI Symbol;Acc:MGI:87876]
ENSMUSG(	Epha5	5:8405476	0.754924	0.077021	-3.29301	down	0.00035	0.005412	Eph receptor A5 [Source:MGI Symbol;Acc:MGI:99654]
ENSMUSG(	Tmem255b	8:1343545	9.87539	1.00777	-3.29267	down	0.0006	0.008131	transmembrane protein 255B [Source:MGI Symbol;Acc:MGI:268553
ENSMUSG(	Srcin1	11:975093	1.2712	0.130626	-3.28268	down	0.00245	0.022975	SRC kinase signaling inhibitor 1 [Source:MGI Symbol;Acc:MGI:19331
ENSMUSG(	Cplx2	13:543713	43.563	4.49362	-3.27715	down	5.00E-05	0.001113	complexin 2 [Source:MGI Symbol;Acc:MGI:104726]
ENSMUSG(	Dner	1:8436983	5.91854	0.61436	-3.26809	down	5.00E-05	0.001113	delta/notch-like EGF repeat containing [Source:MGI Symbol;Acc:MG
ENSMUSG(	Scg3	9:7564326	9.35677	0.975342	-3.26203	down	5.00E-05	0.001113	secretogranin III [Source:MGI Symbol;Acc:MGI:103032]
ENSMUSG(	Kcna6	6:1267083	1.88326	0.19631	-3.26203	down	0.006	0.04479	potassium voltage-gated channel, shaker-related, subfamily, memb
ENSMUSG(	Cckar	5:5369777	1.78806	0.187781	-3.25127	down	0.0003	0.004792	cholecystokinin A receptor [Source:MGI Symbol;Acc:MGI:99478]
ENSMUSG(	Sphkap	1:8325413	2.92149	0.307384	-3.24859	down	0.0014	0.015104	SPHK1 interactor, AKAP domain containing [Source:MGI Symbol;Acc
ENSMUSG(	Astn1	1:1583622	3.21253	0.338255	-3.24753	down	5.00E-05	0.001113	astrotactin 1 [Source:MGI Symbol;Acc:MGI:1098567]
ENSMUSG(	Nrxn1	17:900336	1.23591	0.130511	-3.24333	down	5.00E-05	0.001113	neurexin I [Source:MGI Symbol;Acc:MGI:1096391]
ENSMUSG(	Disp2	2:1187797	3.19338	0.337412	-3.2425	down	5.00E-05	0.001113	dispatched homolog 2 (Drosophila) [Source:MGI Symbol;Acc:MGI:2
ENSMUSG(	Elavl4	4:1102037	7.48142	0.790832	-3.24187	down	5.00E-05	0.001113	ELAV (embryonic lethal, abnormal vision, Drosophila)-like 4 (Hu anti
ENSMUSG(	Syngr3	17:246850	6.99655	0.74119	-3.23873	down	0.0004	0.005949	synaptogyrin 3 [Source:MGI Symbol;Acc:MGI:1341881]
ENSMUSG(	Coro6	11:774624	5.74602	0.612841	-3.22898	down	0.00075	0.009525	coronin 6 [Source:MGI Symbol;Acc:MGI:2183448]
ENSMUSG(	Rbfox3	11:118489	1.65052	0.177057	-3.22064	down	0.0001	0.001959	RNA binding protein, fox-1 homolog (C. elegans) 3 [Source:MGI Sym
ENSMUSG(	Mapk10	5:1029079	6.94157	0.746306	-3.21742	down	0.00065	0.00857	mitogen-activated protein kinase 10 [Source:MGI Symbol;Acc:MGI:1
ENSMUSG(	Lsamp	16:399843	1.59534	0.171863	-3.21454	down	5.00E-05	0.001113	limbic system-associated membrane protein [Source:MGI Symbol;A
ENSMUSG(	Atp2b2	6:1137438	0.766817	0.082839	-3.2105	down	0.0004	0.005949	ATPase, Ca++ transporting, plasma membrane 2 [Source:MGI Symbo
ENSMUSG(	Syt1	10:108497	9.08007	0.984143	-3.20576	down	5.00E-05	0.001113	synaptotagmin I [Source:MGI Symbol;Acc:MGI:99667]
ENSMUSG(	Cacna1g	11:944083	5.7534	0.625859	-3.20051	down	5.00E-05	0.001113	calcium channel, voltage-dependent, T type, alpha 1G subunit [Sour
ENSMUSG(	Kcnq2	2:1810755	1.38552	0.150957	-3.19822	down	5.00E-05	0.001113	potassium voltage-gated channel, subfamily Q, member 2 [Source:M
ENSMUSG(	Vwc2	11:111142	4.39141	0.486426	-3.17439	down	0.0011	0.012657	von Willebrand factor C domain containing 2 [Source:MGI Symbol;A
ENSMUSG(	Lama2	10:269800	2.75276	0.304971	-3.17413	down	5.00E-05	0.001113	laminin, alpha 2 [Source:MGI Symbol;Acc:MGI:99912]
ENSMUSG(	Krt222	11:992327	0.8763	0.097175	-3.17277	down	0.0034	0.029484	keratin 222 [Source:MGI Symbol;Acc:MGI:2442728]
ENSMUSG(	Tacr3	3:1348290	0.866639	0.096184	-3.17156	down	0.0065	0.047385	tachykinin receptor 3 [Source:MGI Symbol;Acc:MGI:892968]
ENSMUSG(	2900011O0	16:139817	2.97108	0.331116	-3.16558	down	0.0015	0.015983	RIKEN cDNA 2900011O08 gene [Source:MGI Symbol;Acc:MGI:19145
ENSMUSG(	Klhl33	14:508913	3.05224	0.341499	-3.15991	down	0.00135	0.01478	kelch-like 33 [Source:MGI Symbol;Acc:MGI:3644593]
ENSMUSG(	Grm7	6:1106397	1.22593	0.137896	-3.15222	down	0.00085	0.010363	glutamate receptor, metabotropic 7 [Source:MGI Symbol;Acc:MGI:1
ENSMUSG(	Rab3c	13:110054	6.64701	0.749369	-3.14896	down	5.00E-05	0.001113	RAB3C, member RAS oncogene family [Source:MGI Symbol;Acc:MG
ENSMUSG(	Lrrc10b	19:104553	18.4696	2.08344	-3.14811	down	5.00E-05	0.001113	leucine rich repeat containing 10B [Source:MGI Symbol;Acc:MGI:26

316]
lex locus [Source:MGI Symbol;Acc:MGI:95777
59021]
:Acc:MGI:97385]
2 [Source:MGI Symbol;Acc:MGI:2159649

l;Acc:MGI:3041196]

Symbol;Acc:MGI:2441996]
i000466]
Acc:MGI:107636]
]
mbol;Acc:MGI:1201400]
444306]
Acc:MGI:1345149]

ce:MGI Symbol;Acc:MGI:104755]
Acc:MGI:1916602
2]
4]
GI:1341818]

ol;Acc:MGI:1932136
MGI:94866
47056]
l Symbol;Acc:MGI:1927126

13]
iI:99444]
643623]

5]
MGI:2441837]
]
mbol;Acc:MGI:102805]
628]

member 14 [Source:MGI Symbol;Acc:MGI:3040688

e:MGI Symbol;Acc:MGI:2385330
mbol;Acc:MGI:2665170

:MGI Symbol;Acc:MGI:1932545]
igen C) [Source:MGI Symbol;Acc:MGI:109157

\cc:MGI:1933407]
926321]

33]
L79]

3I:2152889]

er 6 [Source:MGI Symbol;Acc:MGI:96663]

::MGI:1924879]

388733]
igen D) [Source:MGI Symbol;Acc:MGI:107427

ıbol;Acc:MGI:106368]
1346863]
.cc:MGI:1261760]
ol;Acc:MGI:105368]

ce:MGI Symbol;Acc:MGI:1201678
MGI Symbol;Acc:MGI:1309503]
\cc:MGI:2442987

504]

1351344]
I:1914545]
85551]

GeneID	GeneName	GenePos	Normal_FP	CIP_FPKM	log2(CIP/N	up-or-d	p_value	q_value	Description
NR4A3	NR4A3	chr9:99821	8.07265	0.887981	-3.18444	down	5.00E-05	0.008881	nuclear receptor subfamily 4 group A member 3
PDE3B	PDE3B	chr11:1464	17.1587	2.01877	-3.08739	down	5.00E-05	0.008881	phosphodiesterase 3B
SLC30A1	SLC30A1	chr1:21157	28.4339	3.55831	-2.99835	down	5.00E-05	0.008881	solute carrier family 30 member 1
NR4A2	NR4A2	chr2:15632	9.45282	1.26589	-2.90059	down	5.00E-05	0.008881	nuclear receptor subfamily 4 group A member 2
MAFIP	MAFIP	chr14_GL0	12.7561	1.88814	-2.75615	down	0.00035	0.02913	MAFF interacting protein (pseudogene)
GNAS	GNAS	chr20:5881	231.445	34.279	-2.75527	down	0.0004	0.030825	GNAS complex locus
DUSP5	DUSP5	chr10:1104	33.5931	5.38674	-2.64068	down	5.00E-05	0.008881	dual specificity phosphatase 5
RNF138	RNF138	chr18:3209	4.01929	0.707356	-2.50643	down	0.00035	0.02913	ring finger protein 138
AARD	AARD	chr8:11693	18.1795	3.5028	-2.37573	down	5.00E-05	0.008881	alanine and arginine rich domain containing protein
EGR1	EGR1	chr5:13846	652.389	129.013	-2.33821	down	0.00075	0.045706	early growth response 1
OR51E2	OR51E2	chr11:468(	7.72371	1.57302	-2.29576	down	0.00015	0.018834	olfactory receptor family 51 subfamily E member 2
PTGS2	PTGS2	chr1:18667	12.3364	2.59707	-2.24796	down	5.00E-05	0.008881	prostaglandin-endoperoxide synthase 2
QPCT	QPCT	chr2:37344	27.8446	6.0412	-2.20449	down	0.0001	0.014141	glutaminyl-peptide cyclotransferase
HPGD	HPGD	chr4:17449	35.3531	7.87793	-2.16595	down	0.0001	0.014141	hydroxyprostaglandin dehydrogenase 15-(NAD)
ACTA2	ACTA2	chr10:8893	85.5376	19.424	-2.13872	down	5.00E-05	0.008881	actin, alpha 2, smooth muscle, aorta
FRAS1	FRAS1	chr4:78057	4.30193	0.976974	-2.13859	down	5.00E-05	0.008881	Fraser extracellular matrix complex subunit 1
PLCB1	PLCB1	chr20:8132	4.31585	0.997401	-2.1134	down	0.0001	0.014141	phospholipase C beta 1
LSAMP	LSAMP	chr3:1158(	8.36418	1.98447	-2.07547	down	0.0002	0.022758	limbic system-associated membrane protein
SLC19A2	SLC19A2	chr1:16946	7.66855	1.83741	-2.06128	down	5.00E-05	0.008881	solute carrier family 19 member 2
PTCHD1	PTCHD1	chrX:23334	4.90954	1.17847	-2.05868	down	0.00025	0.025112	patched domain containing 1
ZMAT1	ZMAT1	chrX:10188	4.43891	1.06789	-2.05544	down	0.0002	0.022758	zinc finger matrin-type 1
HAND2-AS	HAND2-AS	chr4:17353	40.6058	9.78601	-2.05289	down	0.0004	0.030825	HAND2 antisense RNA 1 (head to head)
WNT5B	WNT5B	chr12:1617	53.886	13.1592	-2.03384	down	5.00E-05	0.008881	Wnt family member 5B
BCHE	BCHE	chr3:16577	55.867	13.8347	-2.01371	down	5.00E-05	0.008881	butyrylcholinesterase
SCN7A	SCN7A	chr2:1664(	15.2822	3.78544	-2.01332	down	5.00E-05	0.008881	sodium voltage-gated channel alpha subunit 7
LYPLA1	LYPLA1	chr8:54046	8.81139	2.18853	-2.00941	down	0.0006	0.040272	lysophospholipase I
FOXP2	FOXP2	chr7:11408	12.505	3.19461	-1.9688	down	0.00015	0.018834	forkhead box P2
KITLG	KITLG	chr12:8849	10.1904	2.69558	-1.91855	down	5.00E-05	0.008881	KIT ligand
NR4A1	NR4A1	chr12:5202	390.24	103.523	-1.91441	down	0.0003	0.027831	nuclear receptor subfamily 4 group A member 1
MAP4K3	MAP4K3	chr2:39249	6.88301	1.83833	-1.90464	down	5.00E-05	0.008881	mitogen-activated protein kinase kinase kinase kinase 3
BMP3	BMP3	chr4:8103(	10.6939	2.87868	-1.89331	down	5.00E-05	0.008881	bone morphogenetic protein 3
STON1	STON1	chr2:48529	27.0964	7.37748	-1.8769	down	5.00E-05	0.008881	stonin 1
FOXF1	FOXF1	chr16:8651	76.6359	20.9545	-1.87076	down	5.00E-05	0.008881	forkhead box F1

FMOD	FMOD	chr1:20334	340.203	93.8809	-1.85749	down	0.0001	0.014141	fibromodulin
RICTOR	RICTOR	chr5:38937	2.63171	0.752157	-1.80689	down	0.0004	0.030825	RPTOR independent companion of MTOR complex 2
AGL	AGL	chr1:9985(	3.62197	1.03743	-1.80377	down	5.00E-05	0.008881	amylo-alpha-1, 6-glucosidase, 4-alpha-glucanotransferase
HIPK3	HIPK3	chr11:3325	12.4161	3.58939	-1.79041	down	5.00E-05	0.008881	homeodomain interacting protein kinase 3
NEK7	NEK7	chr1:19815	20.0131	5.84839	-1.77483	down	5.00E-05	0.008881	NIMA related kinase 7
LINC01578	LINC01578	chr15:9288	30.8747	9.35966	-1.7219	down	0.00035	0.02913	long intergenic non-protein coding RNA 1578
TMEM106E	TMEM106E	chr7:12211	6.27259	1.90422	-1.71986	down	5.00E-05	0.008881	transmembrane protein 106B
CSRNP1	CSRNP1	chr3:39141	61.812	18.7779	-1.71885	down	5.00E-05	0.008881	cysteine and serine rich nuclear protein 1
EDIL3	EDIL3	chr5:8394(	12.6445	3.86099	-1.71147	down	0.0004	0.030825	EGF like repeats and discoidin domains 3
SEMA3C	SEMA3C	chr7:80742	29.5322	9.07821	-1.70181	down	5.00E-05	0.008881	semaphorin 3C
OSBPL8	OSBPL8	chr12:7635	3.63849	1.11894	-1.70121	down	0.0006	0.040272	oxysterol binding protein like 8
PKN2	PKN2	chr1:88537	4.97471	1.53567	-1.69574	down	0.0001	0.014141	protein kinase N2
TNFAIP3	TNFAIP3	chr6:13782	18.301	5.71698	-1.67859	down	0.00015	0.018834	TNF alpha induced protein 3
PHIP	PHIP	chr6:78934	2.95132	0.928479	-1.66842	down	0.00055	0.038887	pleckstrin homology domain interacting protein
DEK	DEK	chr6:18224	38.8359	12.2863	-1.66033	down	0.0004	0.030825	DEK proto-oncogene
TMEM47	TMEM47	chrX:34627	24.3032	7.69384	-1.65937	down	5.00E-05	0.008881	transmembrane protein 47
KLF10	KLF10	chr8:10264	63.6368	20.2264	-1.65362	down	5.00E-05	0.008881	Kruppel like factor 10
XK	XK	chrX:37685	7.11135	2.2736	-1.64514	down	0.0003	0.027831	X-linked Kx blood group
FAM214A	FAM214A	chr15:5258	5.78118	1.85169	-1.64252	down	0.0005	0.036231	family with sequence similarity 214 member A
AKAP11	AKAP11	chr13:4227	4.74825	1.53387	-1.63022	down	0.00035	0.02913	A-kinase anchoring protein 11
TOX	TOX	chr8:58805	11.3446	3.67069	-1.62788	down	0.00015	0.018834	thymocyte selection associated high mobility group box
DNAJB4	DNAJB4	chr1:78004	16.902	5.48523	-1.62357	down	0.0003	0.027831	DnaJ heat shock protein family (Hsp40) member B4
C5orf24	C5orf24	chr5:13484	12.5016	4.06085	-1.62226	down	0.00015	0.018834	chromosome 5 open reading frame 24
NFIL3	NFIL3	chr9:91409	22.7533	7.4362	-1.61344	down	0.00025	0.025112	nuclear factor, interleukin 3 regulated
PPP1R12A	PPP1R12A	chr12:7977	38.8919	12.7133	-1.61314	down	0.00025	0.025112	protein phosphatase 1 regulatory subunit 12A
SUZ12	SUZ12	chr17:3193	8.47348	2.78914	-1.60313	down	0.00055	0.038887	SUZ12 polycomb repressive complex 2 subunit
PCMTD1	PCMTD1	chr8:51817	20.9551	6.90451	-1.60169	down	0.00025	0.025112	protein-L-isoaspartate (D-aspartate) O-methyltransferase domain containing 1
CCNG1	CCNG1	chr5:16343	33.2684	10.9742	-1.60003	down	0.0006	0.040272	cyclin G1
KCTD12	KCTD12	chr13:7688	25.6854	8.47988	-1.59883	down	0.0002	0.022758	potassium channel tetramerization domain containing 12
CREBRF	CREBRF	chr5:17305	3.74596	1.24739	-1.58643	down	0.00035	0.02913	CREB3 regulatory factor
NBEA	NBEA	chr13:3494	9.64635	3.21563	-1.58488	down	0.0006	0.040272	neurobeachin
ARHGAP5	ARHGAP5	chr14:3207	5.85879	1.95348	-1.58456	down	0.0002	0.022758	Rho GTPase activating protein 5
CTGF	CTGF	chr6:13194	237.665	79.5988	-1.57811	down	0.00015	0.018834	connective tissue growth factor
HLTF	HLTF	chr3:14903	7.97092	2.67159	-1.57705	down	0.0003	0.027831	helicase like transcription factor
MBNL2	MBNL2	chr13:9722	15.7475	5.28051	-1.57638	down	5.00E-05	0.008881	muscleblind like splicing regulator 2

SCOC	SCOC	chr4:14025	24.5154	8.22808	-1.57506	down	0.0005	0.036231	short coiled-coil protein
DUSP10	DUSP10	chr1:2217(	27.0793	9.09672	-1.57377	down	0.0004	0.030825	dual specificity phosphatase 10
CDK17	CDK17	chr12:9627	8.58437	2.89449	-1.5684	down	0.0007	0.044717	cyclin-dependent kinase 17
ZYG11B	ZYG11B	chr1:52726	7.63562	2.58005	-1.56535	down	0.00025	0.025112	zyg-11 family member B, cell cycle regulator
SLC38A2	SLC38A2	chr12:4635	34.4601	11.6757	-1.56142	down	5.00E-05	0.008881	solute carrier family 38 member 2
PTBP2	PTBP2	chr1:96721	27.3603	9.2846	-1.55917	down	0.00015	0.018834	polypyrimidine tract binding protein 2
CD164	CD164	chr6:10936	50.4164	17.1241	-1.55787	down	0.00075	0.045706	CD164 molecule
CITED2	CITED2	chr6:13937	196.735	67.5887	-1.5414	down	0.0007	0.044717	Cbp/p300 interacting transactivator with Glu/Asp rich carboxy-terminal domain
HECA	HECA	chr6:13913	8.47445	2.92519	-1.53459	down	0.00025	0.025112	hdc homolog, cell cycle regulator
ZNF37BP	ZNF37BP	chr10:4251	2.94272	1.02043	-1.52797	down	0.0003	0.027831	zinc finger protein 37B, pseudogene
TBL1XR1	TBL1XR1	chr3:17702	9.56031	3.31771	-1.52687	down	0.00015	0.018834	transducin (beta)-like 1 X-linked receptor 1
ZFP36L1	ZFP36L1	chr14:6878	282.272	100.102	-1.49561	down	0.0008	0.047951	ZFP36 ring finger protein-like 1
RGS1	RGS1	chr1:19257	177.307	63.0348	-1.49203	down	0.00035	0.02913	regulator of G-protein signaling 1
MED13	MED13	chr17:6194	3.10697	1.11642	-1.47663	down	0.0005	0.036231	mediator complex subunit 13
PTAR1	PTAR1	chr9:69709	3.00887	1.08859	-1.46676	down	0.00075	0.045706	protein prenyltransferase alpha subunit repeat containing 1
RAD21	RAD21	chr8:11684	39.4599	14.2923	-1.46515	down	0.0004	0.030825	RAD21 cohesin complex component
DEPTOR	DEPTOR	chr8:11987	23.5023	8.59361	-1.45147	down	0.00015	0.018834	DEP domain containing MTOR-interacting protein
RYR2	RYR2	chr1:23704	2.41657	0.888866	-1.44292	down	0.00015	0.018834	ryanodine receptor 2
PIK3C2A	PIK3C2A	chr11:1708	4.09246	1.50726	-1.44104	down	0.0004	0.030825	phosphatidylinositol-4-phosphate 3-kinase catalytic subunit type 2 alpha
DIXDC1	DIXDC1	chr11:1119	24.8657	9.16516	-1.43993	down	5.00E-05	0.008881	DIX domain containing 1
CNN1	CNN1	chr19:1153	93.0708	34.661	-1.42501	down	0.0002	0.022758	calponin 1
FAM199X	FAM199X	chrX:10416	3.72898	1.39015	-1.42353	down	0.0007	0.044717	family with sequence similarity 199, X-linked
FBXL3	FBXL3	chr13:7700	10.029	3.74573	-1.42086	down	0.00055	0.038887	F-box and leucine rich repeat protein 3
NEGR1	NEGR1	chr1:71402	14.5411	5.43308	-1.4203	down	0.00025	0.025112	neuronal growth regulator 1
ABI3BP	ABI3BP	chr3:10074	11.5529	4.33212	-1.4151	down	0.0003	0.027831	ABI family member 3 binding protein
PDE3A	PDE3A	chr12:2036	12.3429	4.7574	-1.37544	down	0.00045	0.03344	phosphodiesterase 3A
FZD7	FZD7	chr2:20203	50.9623	19.7373	-1.3685	down	0.00035	0.02913	frizzled class receptor 7
GFRA1	GFRA1	chr10:1160	14.8293	5.76533	-1.36297	down	0.00035	0.02913	GDNF family receptor alpha 1
MAMDC2	MAMDC2	chr9_GL38	24.9358	9.7146	-1.35999	down	0.00075	0.045706	MAM domain containing 2
TIPARP	TIPARP	chr3:15667	16.2825	6.39303	-1.34875	down	0.00035	0.02913	TCDD inducible poly(ADP-ribose) polymerase
ZMYM2	ZMYM2	chr13:1995	5.0584	1.98758	-1.34767	down	0.0006	0.040272	zinc finger MYM-type containing 2
BMPR1A	BMPR1A	chr10:8675	24.9213	9.8072	-1.34546	down	0.0004	0.030825	bone morphogenetic protein receptor type 1A
CREB1	CREB1	chr2:20752	12.4786	4.91883	-1.34307	down	0.0006	0.040272	cAMP responsive element binding protein 1
RERG	RERG	chr12:1510	37.1528	14.6671	-1.34089	down	0.0007	0.044717	RAS like estrogen regulated growth inhibitor
THUMPD1	THUMPD1	chr16:2073	18.1363	7.20653	-1.3315	down	0.00055	0.038887	THUMP domain containing 1

PCNP	PCNP	chr3:10157	52.2783	20.8636	-1.32523	down	0.0007	0.044717	PEST proteolytic signal containing nuclear protein
PDZRN4	PDZRN4	chr12:4118	22.0272	8.79096	-1.32519	down	0.00075	0.045706	PDZ domain containing ring finger 4
NFYB	NFYB	chr12:1041	17.3467	6.95836	-1.31784	down	0.0007	0.044717	nuclear transcription factor Y subunit beta
SLC8A1	SLC8A1	chr2:39917	19.6948	7.90552	-1.31689	down	0.00075	0.045706	solute carrier family 8 member A1
LBR	LBR	chr1:2254(	41.8595	16.9577	-1.30361	down	0.0005	0.036231	lamin B receptor
PHLDB2	PHLDB2	chr3:11167	16.5465	6.80205	-1.28249	down	0.00035	0.02913	pleckstrin homology like domain family B member 2
RNF11	RNF11	chr1:51236	31.444	12.9697	-1.27764	down	0.00055	0.038887	ring finger protein 11
TJP1	TJP1	chr15_KI27	17.2662	7.48493	-1.20589	down	0.00075	0.045706	tight junction protein 1
TUBA1C	TUBA1C	chr12:4922	32.0693	78.79	1.29682	up	0.00025	0.025112	tubulin alpha 1c
KRT8	KRT8	chr12:5289	83.3636	208.32	1.32131	up	0.0006	0.040272	keratin 8
CRIP2	CRIP2	chr14:1054	101.247	253.302	1.32298	up	0.00035	0.02913	cysteine rich protein 2
MFGE8	MFGE8	chr15:8889	41.1236	104.026	1.33891	up	0.0004	0.030825	milk fat globule-EGF factor 8 protein
RRBP1	RRBP1	chr20:1761	17.6307	45.6263	1.37178	up	0.0001	0.014141	ribosome binding protein 1
PMM2	PMM2	chr16:8797	5.7784	15.0764	1.38355	up	0.0007	0.044717	phosphomannomutase 2
CRIP1	CRIP1	chr14:1054	124.503	325.468	1.38634	up	0.00075	0.045706	cysteine rich protein 1
APOL1	APOL1	chr22:3625	14.9029	39.0253	1.38882	up	0.0006	0.040272	apolipoprotein L1
THBS3	THBS3	chr1:15519	10.8497	28.6472	1.40075	up	0.00025	0.025112	thrombospondin 3
ANXA2	ANXA2	chr15:6034	107.205	286.924	1.4203	up	0.00035	0.02913	annexin A2
TMSB10	TMSB10	chr2:84905	1148.78	3121.07	1.44193	up	0.0005	0.036231	thymosin beta 10
PECAM1	PECAM1	chr17:6431	10.1723	27.9129	1.45628	up	0.00075	0.045706	platelet and endothelial cell adhesion molecule 1
SH3RF3	SH3RF3	chr2:10912	3.49992	9.80312	1.48592	up	0.00075	0.045706	SH3 domain containing ring finger 3
S100A11	S100A11	chr1:15203	225.606	640.55	1.50551	up	0.0002	0.022758	S100 calcium binding protein A11
SYNPO	SYNPO	chr5:1506(	15.5497	44.2557	1.50898	up	0.00035	0.02913	synaptopodin
SULF2	SULF2	chr20:4765	21.9617	62.998	1.52032	up	0.0001	0.014141	sulfatase 2
ADAMTS7	ADAMTS7	chr15:7875	3.32233	9.53227	1.52062	up	0.0003	0.027831	ADAM metallopeptidase with thrombospondin type 1 motif 7
RNASE1	RNASE1	chr14:208(	57.2389	164.6	1.5239	up	0.00025	0.025112	ribonuclease A family member 1, pancreatic
PENK	PENK	chr8:5644(	46.1029	133.128	1.52989	up	0.00025	0.025112	proenkephalin
DDIT4	DDIT4	chr10:7227	24.2181	70.228	1.53596	up	0.0001	0.014141	DNA damage inducible transcript 4
RASSF2	RASSF2	chr20:478(	4.88815	14.6465	1.58319	up	0.0004	0.030825	Ras association domain family member 2
CD68	CD68	chr17:7579	8.04409	24.1164	1.58401	up	0.00035	0.02913	CD68 molecule
C1QTNF5	C1QTNF5	chr11:1193	21.7886	65.518	1.58832	up	0.00035	0.02913	C1q and tumor necrosis factor related protein 5
PALMD	PALMD	chr1:99516	2.73909	8.25994	1.59243	up	0.00025	0.025112	palmdelphin
SH3BGRL3	SH3BGRL3	chr1:26279	42.3079	128.001	1.59715	up	5.00E-05	0.008881	SH3 domain binding glutamate rich protein like 3
TMSB4X	TMSB4X	chrX:12975	1382.9	4238.58	1.61589	up	0.0008	0.047951	thymosin beta 4, X-linked
ARHGDIB	ARHGDIB	chr12:1494	28.4789	87.8239	1.62472	up	0.00015	0.018834	Rho GDP dissociation inhibitor beta

FAM101B	FAM101B	chr17:4399	9.15295	28.2422	1.62554	up	0.00025	0.025112	family with sequence similarity 101 member B
PCSK1N	PCSK1N	chrX:48831	138.861	429.206	1.62803	up	0.0006	0.040272	proprotein convertase subtilisin/kexin type 1 inhibitor
SCRG1	SCRG1	chr4:17338	42.4913	131.446	1.62923	up	5.00E-05	0.008881	stimulator of chondrogenesis 1
FMOD	FMOD	chr1:20334	14.8466	46.2497	1.63931	up	0.0001	0.014141	fibromodulin
HOXB7	HOXB7	chr17:486(	10.5291	33.0215	1.64903	up	0.00065	0.042838	homeobox B7
LAPTM5	LAPTM5	chr1:30732	13.8606	43.7432	1.65807	up	5.00E-05	0.008881	lysosomal protein transmembrane 5
PCOLCE	PCOLCE	chr7:10058	11.2288	36.1908	1.68842	up	0.0003	0.027831	procollagen C-endopeptidase enhancer
ENG	ENG	chr9:12781	13.6305	44.0979	1.69387	up	5.00E-05	0.008881	endoglin
HN1	HN1	chr17:7513	5.9656	19.5906	1.71542	up	0.00065	0.042838	hematological and neurological expressed 1
C1QC	C1QC	chr1:22643	42.6492	140.69	1.72193	up	0.0001	0.014141	complement component 1, q subcomponent, C chain
DNAJA4	DNAJA4	chr15:7826	9.63118	31.8609	1.726	up	0.0002	0.022758	DnaJ heat shock protein family (Hsp40) member A4
FABP3	FABP3	chr1:31365	12.1757	40.5896	1.73711	up	0.0004	0.030825	fatty acid binding protein 3
ATP10A	ATP10A	chr15:2567	2.06634	7.00679	1.76168	up	0.0002	0.022758	ATPase phospholipid transporting 10A (putative)
SCG2	SCG2	chr2:22359	11.024	37.5289	1.76735	up	5.00E-05	0.008881	secretogranin II
CFB	CFB	chr6_GL00(	2.89889	10.0215	1.78953	up	0.00045	0.03344	complement factor B
C1QB	C1QB	chr1:22653	53.212	185.692	1.80309	up	5.00E-05	0.008881	complement component 1, q subcomponent, B chain
RFTN1	RFTN1	chr3:16315	5.54028	19.6144	1.82388	up	5.00E-05	0.008881	raftlin, lipid raft linker 1
VWF	VWF	chr12:5948	6.92874	24.7842	1.83876	up	5.00E-05	0.008881	von Willebrand factor
TAC3	TAC3	chr12:5700	17.4152	62.7334	1.84888	up	0.0004	0.030825	tachykinin 3
CYFIP2	CYFIP2	chr5:15726	3.96529	14.4606	1.86663	up	5.00E-05	0.008881	cytoplasmic FMR1 interacting protein 2
IL32	IL32	chr16:3065	24.2631	89.9137	1.88977	up	0.0002	0.022758	interleukin 32
ISG15	ISG15	chr1:10134	158.276	595.455	1.91155	up	0.0001	0.014141	ISG15 ubiquitin-like modifier
S100A10	S100A10	chr1:15198	110	417.469	1.92416	up	5.00E-05	0.008881	S100 calcium binding protein A10
KCNE4	KCNE4	chr2:22305	4.59874	17.4704	1.9256	up	0.0001	0.014141	potassium voltage-gated channel subfamily E regulatory subunit 4
CASQ1	CASQ1	chr1:16019	6.25794	24.2525	1.95438	up	5.00E-05	0.008881	calsequestrin 1
PDPN	PDPN	chr1:13583	3.59821	14.2307	1.98365	up	0.00015	0.018834	podoplanin
CFD	CFD	chr19_KI27	35.0889	139.132	1.98737	up	0.0001	0.014141	complement factor D
THY1	THY1	chr11:1193	46.2213	184.463	1.9967	up	5.00E-05	0.008881	Thy-1 cell surface antigen
SFRP2	SFRP2	chr4:15378	10.5038	42.904	2.0302	up	0.0001	0.014141	secreted frizzled related protein 2
CCNB1	CCNB1	chr5:69167	1.70715	7.37951	2.11193	up	0.00025	0.025112	cyclin B1
HSPB3	HSPB3	chr5:54455	13.8157	59.9987	2.11862	up	5.00E-05	0.008881	heat shock protein family B (small) member 3
CARTPT	CARTPT	chr5:71719	52.5701	230.835	2.13455	up	5.00E-05	0.008881	CART prepropeptide
RSPO1	RSPO1	chr1:37611	0.898916	3.98393	2.14794	up	0.00035	0.02913	R-spondin 1
TAC1	TAC1	chr7:97731	12.8758	57.4527	2.15772	up	0.0001	0.014141	tachykinin precursor 1
HOXC8	HOXC8	chr12:540(	8.1787	36.9997	2.17757	up	5.00E-05	0.008881	homeobox C8

CDC20	CDC20	chr1:43358	1.81041	8.27972	2.19327	up	0.0008	0.047951	cell division cycle 20
HMGB3	HMGB3	chrX:15098	2.13438	9.87577	2.21008	up	0.0001	0.014141	high mobility group box 3
GIMAP7	GIMAP7	chr7:15051	7.55667	35.3496	2.22587	up	0.0002	0.022758	GTPase, IMAP family member 7
CFI	CFI	chr4:10974	2.10344	9.84906	2.22724	up	0.00065	0.042838	complement factor I
TNFRSF12A	TNFRSF12A	chr16:3020	22.2865	105.45	2.24231	up	5.00E-05	0.008881	tumor necrosis factor receptor superfamily member 12A
NOSTRIN	NOSTRIN	chr2_GL38	0.871167	4.21934	2.276	up	0.00075	0.045706	nitric oxide synthase trafficking
SERPINA3	SERPINA3	chr14:9461	6.32282	30.9332	2.29052	up	5.00E-05	0.008881	serpin family A member 3
ERAP2	ERAP2	chr5:96875	0.566634	2.81965	2.31503	up	5.00E-05	0.008881	endoplasmic reticulum aminopeptidase 2
ELN	ELN	chr7:74027	29.6202	148.023	2.32116	up	5.00E-05	0.008881	elastin
BGN	BGN	chrX:15344	15.6424	78.331	2.32412	up	5.00E-05	0.008881	biglycan
ACTC1	ACTC1	chr15:3475	0.787284	4.01325	2.34982	up	0.0004	0.030825	actin, alpha, cardiac muscle 1
SLCO2A1	SLCO2A1	chr3:13393	2.00832	10.4261	2.37614	up	0.00065	0.042838	solute carrier organic anion transporter family member 2A1
LOXL2	LOXL2	chr8:23296	18.2876	95.849	2.3899	up	5.00E-05	0.008881	lysyl oxidase like 2
PDLIM1	PDLIM1	chr10:9523	37.9666	204.442	2.42889	up	5.00E-05	0.008881	PDZ and LIM domain 1
PRR11	PRR11	chr17:5915	0.228312	1.25751	2.46149	up	0.0003	0.027831	proline rich 11
ACKR1	ACKR1	chr1:1592(	7.88933	43.5015	2.46309	up	5.00E-05	0.008881	atypical chemokine receptor 1 (Duffy blood group)
AURKA	AURKA	chr20:5636	0.823631	4.57624	2.47409	up	0.00035	0.02913	aurora kinase A
IL17B	IL17B	chr5:14937	6.0259	33.5517	2.47714	up	0.0001	0.014141	interleukin 17B
GGT5	GGT5	chr22:2421	2.80845	15.6402	2.47741	up	0.0003	0.027831	gamma-glutamyltransferase 5
CRABP2	CRABP2	chr1:15669	5.54382	32.2564	2.54063	up	5.00E-05	0.008881	cellular retinoic acid binding protein 2
GAL	GAL	chr11:6868	56.252	333.648	2.56835	up	5.00E-05	0.008881	galanin and GMAP prepropeptide
CILP	CILP	chr15:6519	3.46357	20.7534	2.58302	up	5.00E-05	0.008881	cartilage intermediate layer protein
KIF2C	KIF2C	chr1:44739	0.533802	3.25533	2.60843	up	0.0002	0.022758	kinesin family member 2C
FCGR3A	FCGR3A	chr1:16154	1.86307	11.7469	2.65653	up	5.00E-05	0.008881	Fc fragment of IgG receptor IIIa
PLVAP	PLVAP	chr19:1735	9.76742	62.5016	2.67784	up	5.00E-05	0.008881	plasmalemma vesicle associated protein
CCL14	CCL14	chr17_KI27	69.9137	483.197	2.78897	up	5.00E-05	0.008881	C-C motif chemokine ligand 14
IGFBP2	IGFBP2	chr2:21663	36.5675	252.952	2.79023	up	5.00E-05	0.008881	insulin like growth factor binding protein 2
INMT	INMT	chr7:30752	4.57495	32.9864	2.85004	up	0.0001	0.014141	indolethylamine N-methyltransferase
ZNF469	ZNF469	chr16:8842	0.161058	1.1857	2.88009	up	0.0003	0.027831	zinc finger protein 469
TOP2A	TOP2A	chr17:4038	0.262533	1.93615	2.88262	up	0.00045	0.03344	topoisomerase (DNA) II alpha
PLXNA4	PLXNA4	chr7:13212	0.556563	4.22768	2.92525	up	5.00E-05	0.008881	plexin A4
INHBB	INHBB	chr2:12034	0.64523	5.04394	2.96667	up	0.0001	0.014141	inhibin beta B subunit
SPAG5	SPAG5	chr17:2857	0.256339	2.02985	2.98524	up	0.00045	0.03344	sperm associated antigen 5
TK1	TK1	chr17:7817	2.91077	23.5328	3.0152	up	5.00E-05	0.008881	thymidine kinase 1
NNMT	NNMT	chr11:1142	11.9934	100.117	3.06138	up	5.00E-05	0.008881	nicotinamide N-methyltransferase

CDHR3	CDHR3	chr7:10596	1.6832	14.1468	3.0712	up	5.00E-05	0.008881	cadherin related family member 3
STC2	STC2	chr5:17331	2.36748	21.8563	3.20663	up	5.00E-05	0.008881	stanniocalcin 2
BASP1	BASP1	chr5:1713(	13.7084	129.034	3.23462	up	5.00E-05	0.008881	brain abundant membrane attached signal protein 1
EZH2	EZH2	chr7:1488(	0.242594	2.33178	3.26482	up	0.00025	0.025112	enhancer of zeste 2 polycomb repressive complex 2 subunit
KIF4A	KIF4A	chrX:7029(	0.095145	0.939197	3.30323	up	0.0003	0.027831	kinesin family member 4A
CENPM	CENPM	chr22:4193	0.563969	5.75995	3.35237	up	0.00045	0.03344	centromere protein M
STC1	STC1	chr8:23841	0.398066	4.19468	3.39748	up	0.0001	0.014141	stanniocalcin 1
ARHGAP11	ARHGAP11	chr15_KI27	0.133995	1.46329	3.44897	up	5.00E-05	0.008881	Rho GTPase activating protein 11A
CDKN3	CDKN3	chr14:5439	1.64388	18.349	3.48052	up	5.00E-05	0.008881	cyclin-dependent kinase inhibitor 3
SERPINE1	SERPINE1	chr7:10112	2.4409	28.0905	3.5246	up	5.00E-05	0.008881	serpin family E member 1
GPBAR1	GPBAR1	chr2:21826	8.0299	95.8646	3.57754	up	5.00E-05	0.008881	G protein-coupled bile acid receptor 1
TGFBI	TGFBI	chr5:13602	28.5975	341.666	3.57862	up	5.00E-05	0.008881	transforming growth factor beta induced
MYH3	MYH3	chr17:1062	0.780314	9.64707	3.62796	up	5.00E-05	0.008881	myosin, heavy chain 3, skeletal muscle, embryonic
KIFC1	KIFC1	chr6_GL00(	0.236575	3.00897	3.6689	up	0.0002	0.022758	kinesin family member C1
OXTR	OXTR	chr3:87504	0.122934	1.57727	3.68147	up	0.00025	0.025112	oxytocin receptor
P4HA3	P4HA3	chr11:7426	0.489528	6.79631	3.79529	up	5.00E-05	0.008881	prolyl 4-hydroxylase subunit alpha 3
F2RL3	F2RL3	chr19:1688	0.544302	8.37135	3.94298	up	5.00E-05	0.008881	F2R like thrombin/trypsin receptor 3
PTTG1	PTTG1	chr5:16042	3.18179	50.4266	3.98628	up	5.00E-05	0.008881	pituitary tumor-transforming 1
ODAM	ODAM	chr4:70196	3.93648	67.1768	4.09298	up	5.00E-05	0.008881	odontogenic, ameloblast asssociated
CCNB2	CCNB2	chr15:591(	0.329726	6.35923	4.26951	up	0.0001	0.014141	cyclin B2
HJURP	HJURP	chr2:23383	0.132275	2.65133	4.3251	up	0.00025	0.025112	Holliday junction recognition protein
CENPF	CENPF	chr1:2146(	0.076165	1.6374	4.42613	up	5.00E-05	0.008881	centromere protein F
LAMC2	LAMC2	chr1:18318	0.135117	3.0815	4.51136	up	5.00E-05	0.008881	laminin subunit gamma 2
CEP55	CEP55	chr10:9349	0.278794	6.37217	4.51451	up	0.0006	0.040272	centrosomal protein 55
CACNG4	CACNG4	chr17:6696	0.349943	8.71616	4.6385	up	5.00E-05	0.008881	calcium voltage-gated channel auxiliary subunit gamma 4
IQGAP3	IQGAP3	chr1:15652	0.091629	2.3642	4.6894	up	0.00035	0.02913	IQ motif containing GTPase activating protein 3
PRSS12	PRSS12	chr4:11828	0.148093	4.10339	4.79224	up	0.0006	0.040272	protease, serine 12
C8orf37-AS	C8orf37-AS	chr8:95244	0.208944	7.09637	5.08589	up	0.0001	0.014141	C8orf37 antisense RNA 1

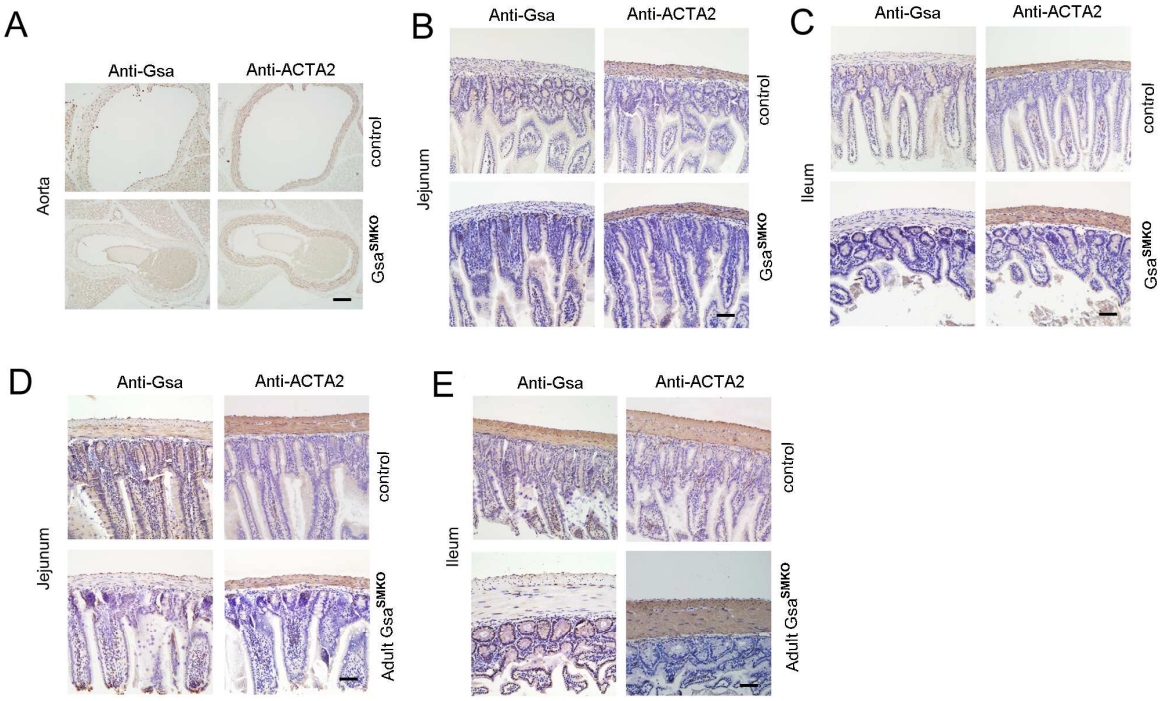

Supplementary Figure 1. Acta2-Cre or SM22-CreER^{T2} mediated Gsa knockout happened in smooth muscle layer. A-C, Immunohistochemistry of Gsa and ACTA2 in cross sections of aorta (**A**), jejunum (**B**) and ileum (**C**) from control and Gsa^{SMKO} mice. Scale bars in panel A represent 500 μm; scale bars in panel B and C represent 50 μm. **D-E**, Immunohistochemistry of Gsa and ACTA2 in cross sections of jejunum (**D**) and ileum (**E**) from control and adult Gsa^{SMKO} mice. Scale bars in panel D and E represent 50 μm.

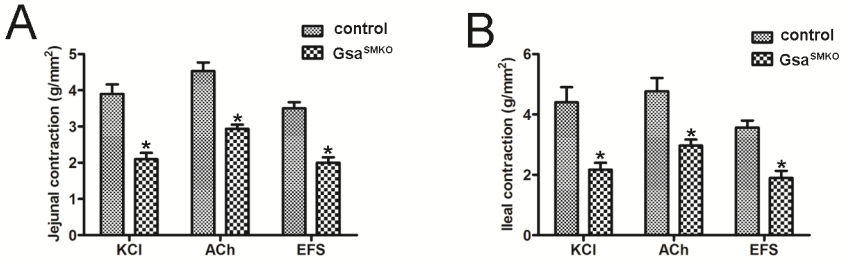

Supplementary Figure 2. Gsa knockout in smooth muscle impaired contraction. A and **B**, The jejunum (**A**) and ileum (**B**) from control and Gsa^{SMKO} mice at 13 days was treated with 87 mM KCl, 1 μM ACh or electrical field stimulation (EFS) (20 Hz, 30 V, pulse train, 20 s) followed by quantitative analysis (n=5). * $p < 0.05$ *vs* control.

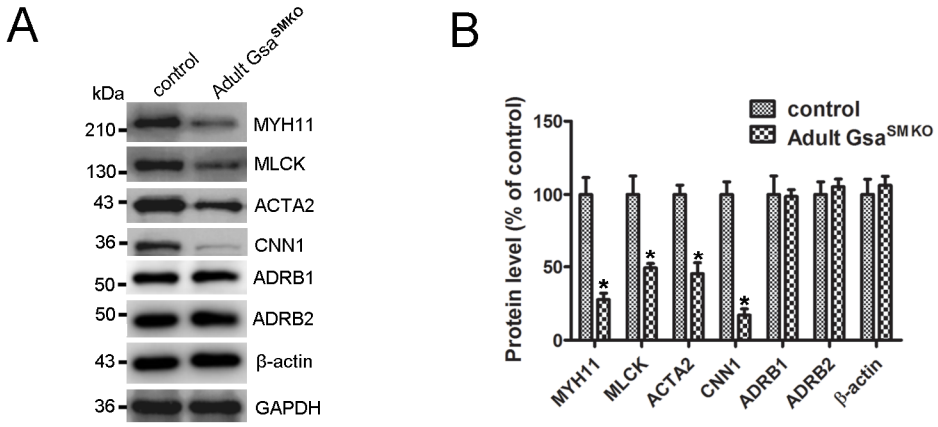

Supplementary Figure 3. Gsa deletion in smooth muscle reduced the expression of contractile proteins. A, Western blot analysis of the levels of contractile proteins from control and adult Gsa^{SMKO} mice. **B**, Quantitative analysis of the levels of contractile proteins from control and adult Gsa^{SMKO} mice (n=4). * $p < 0.05$ *vs* control.

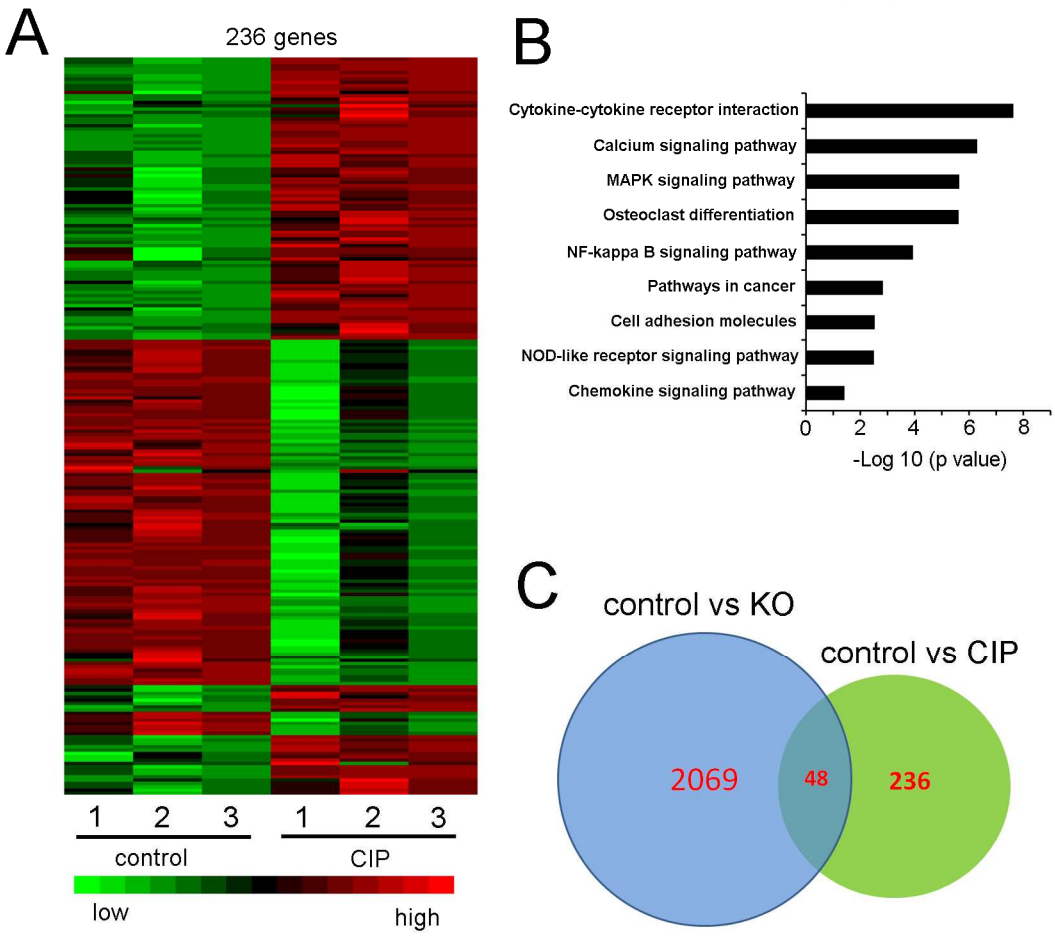

D

Gene Name	Description
ANXA2	annexin A2
ARHGDIB	Rho GDP dissociation inhibitor beta
ATP10A	ATPase phospholipid transporting 10A (putative)
C1QB	complement component 1, q subcomponent, B chain
CCNB1	cyclin B1
CD68	CD68 molecule
DDIT4	DNA damage inducible transcript 4
ISG15	ISG15 ubiquitin-like modifier
KCNE4	potassium voltage-gated channel subfamily E regulatory subunit 4
KRT8	keratin 8
LAMC2	laminin subunit gamma 2
NNMT	nicotinamide N-methyltransferase
PALMD	palmdelphin
PDPN	podoplanin
RFTN1	raftlin, lipid raft linker 1
S100A10	S100 calcium binding protein A10
S100A11	S100 calcium binding protein A11
SERPINE1	serpin family E member 1
SH3BGRL3	SH3 domain binding glutamate rich protein like 3
TNFRSF12A	tumor necrosis factor receptor superfamily member 12A
TUBA1C	tubulin alpha 1c

E

Gene Name	Description
ACTA2	actin, alpha 2, smooth muscle, aorta
BCHE	butyrylcholinesterase
CDK17	cyclin-dependent kinase 17
CNN1	calponin 1
CREB1	cAMP responsive element binding protein 1
EDIL3	EGF like repeats and discoidin domains 3
FAM214A	family with sequence similarity 214 member A
FMOD	fibromodulin
FOXF1	forkhead box F1
FOXP2	forkhead box P2
GNAS	GNAS complex locus
KCTD12	potassium channel tetramerization domain containing 12
LBR	lamin B receptor
LSAMP	limbic system-associated membrane protein
MAMDC2	MAM domain containing 2
PCMTD1	protein-L-isoaspartate (D-aspartate) O-methyltransferase domain containing 1
PDE3A	phosphodiesterase 3A
PHLDB2	pleckstrin homology like domain family B member 2
PLCB1	phospholipase C beta 1
PPP1R12A	protein phosphatase 1 regulatory subunit 12A
QPCT	glutaminyl-peptide cyclotransferase
RERG	RAS like estrogen regulated growth inhibitor
RYR2	ryanodine receptor 2
SCN7A	sodium voltage-gated channel alpha subunit 7
TMEM47	transmembrane protein 47
TOX	thymocyte selection associated high mobility group box
XK	X-linked Kx blood group

Supplementary Figure 4. Microarray analysis of gene expression from human and mice tissues. A, Microarray assay of genes with >2.0-fold upregulation or >2.0-fold downregulation in patients with CIP compared with age-matched control group. **B**, Top 9 enrichment pathways with a significantly changed genes based on the KEGG database. **C**, Venn diagram of differentially expressed genes in patients with CIP compared to control and Gsa KO compared to control found in microarray analysis (>2-fold). **D**, A list of common genes with over 2-fold upregulation both in the groups of patients with CIP and Gsa KO. **E**, A list of common genes with over 2-fold downregulation both in the groups of patients with CIP and Gsa KO.